

RETURNING MATERIALS:
Place in book drop to
remove this checkout from
your record. FINES will
be charged if book is
returned after the date
stamped below.

# MICROBALANCE TECHNIQUES IN ATMOSPHERIC CORROSION

Ву

Jose Luis Flores Milchorena

## A THESIS

Submitted to
Michigan State University
in partial fulfillment of the requirements
for the degree of

MASTER OF SCIENCE

Department of Metallurgy, Mechanics, And Materials Science

1981

## ABSTRACT

# MICROBALANCE TECHNIQUES IN ATMOSPHERIC CORROSION

Ву

## Jose Luis Flores Milchorena

A microbalance system for continuous measurement of atmospheric corrosion was constructed. Short-term corrosion rates were measured for 4340 steel and magnesium alloy AZ31B in moist air, dry sulfur dioxide, and moist sulfur dioxide.

Corrosion rates measured with the microbalance were compared with rates measured in a static environmental chamber. The results show that the continuous microbalance method is a useful technique for rapid corrosion testing.

Con todo cariño y respeto a mis padres Efren y Olga

### ACKNOWLEDGMENTS

I wish to express my sincere appreciation to Dr. Robert Summitt for his valuable guidance and continued assistance throughout the course of the work which made this thesis possible.

# TABLE OF CONTENTS

			Page
List of Ta	ables	•••••	v
List of F	igures .	•••••	vii
Chapter			
ı.	INTRO	DUCTION	1
II.	ATMOS	PHERIC CORROSION OF METALS	5
	A. B.	Types of Atmospheres	8
	ь.	Factors Influencing Corrosivity of the Atmosphere	8
III.	LITER	ATURE REVIEW	18
	А.	Atmospheric Corrosion Studies Involving the Use of Continuous Reading Techniques with Microbalances . Atmospheric Corrosion Studies not Involving Continuous Reading	18
		Techniques	22
IV.	EXPER	IMENTAL PROCEDURE	36
	A. B. C. D.	Equipment	36 44 45 49
v.	RESUL	TS AND DISCUSSION	55
	A. B.	Low Alloy High Strength Steel 4340 Magnesium Alloy AZ31B	55 75
VI.	CONCL	USIONS	97
APPENDIX :	ı	• • • • • • • • • • • • • • • • • • • •	101
፣ ተርጥ <u>በ</u> ዩ ይነ	PEPDEMCE	c	102

# LIST OF TABLES

Table		Page
1.	Seven-year exposure of magnesium alloys in marine atmospheres. Results obtained by Ailor (33)	24
2.	Atmospheric exposure corrosion rates (mm/year) in marine tropical atmospheres. Results obtained by Pelensky and Jaworski (34)	26
3.	Atmospheric exposure corrosion rates (mm/year) in three different air force bases. Results reported by Summitt and Fink (4)	27
4.	Corrosion rates (mm/year) for magnesium alloy AZ31B after four years exposure in the Panama Canal Zone. Results reported by Pearlstein and Teitell (35)	28
5.	Saturation solubilities in water and relative humidities of lithium nitrate, sodium chloride and lead nitrate at various temperatures	43
6.	Chemical composition of low alloy high strength steel 4340 (%)	46
7.	Chemical composition of magnesium alloy AZ31B (%)	48
8.	Values of weight gain, weight loss and corrosion rate for 4340 steel in the presence of moist air (49% R.H.). Microbalance and chamber results	59
9.	Values of weight gain, weight loss and corrosion rate for 4340 steel in the presence of moist air (75% R.H.). Microbalance and chamber results	60
10.	Values of weight gain, weight loss and corrosion rate for 4340 steel in the presence of moist air (98% R.H.). Microbalance and chamber results	61
11.	Values of weight gain, weight loss and corrosion rate for 4340 steel in the presence of dry SO <sub>2</sub> .	67

Table		Page
12.	Values of weight gain, weight loss and corrosion rate for 4340 steel in the presence of moist SO <sub>2</sub> (49% R.H.). Microbalance and chamber results	71
13.	Values of weight gain, weight loss and corrosion rate for 4340 steel in the presence of moist SO 2 (98% R.H.). Microbalance and chamber results	72
14.	Values of weight gain, weight loss and corrosion rate for magnesium AZ31B in the presence of moist air (49% R.H.). Microbalance and chamber results	78
15.	Values of weight gain, weight loss and corrosion rate for magnesium AZ31B in the presence of moist air (75% R.H.). Microbalance and chamber results	79
16.	Values of weight gain, weight loss and corrosion rate for magnesium AZ31B in the presence of moist air (98% R.H.). Microbalance and chamber results	80
17.	Values of weight gain, weight loss and corrosion rate for magnesium AZ31B in the presence of dry SO <sub>2</sub> . Microbalance and chamber results	85
18.	Values of weight gain, weight loss and corrosion rate for magnesium AZ31B in the presence of moist SO <sub>2</sub> (49% R.H.). Microbalance and chamber results	90
19.	Values of weight gain, weight loss and corrosion rate for magnesium AZ31B in the presence of moist SO <sub>2</sub> (98% R.H.). Microbalance and chamber results	91
20.	Comparisons between the results obtained in this experiment and the results reported by Pelensky and Jaworski (34) and Summitt and Fink (4) for 4340 steel	95
21.	Comparisons between the results obtained in this experiment and the results reported by Pelensky and Jaworski (34) and Summitt and Fink (4) for magnesium A731B	96

# LIST OF FIGURES

Figure		Page
1.	Dependence of atmospheric corrosion on the amount of surface moisture (1)	7
2.	Effect of the protective properties of the corrosion products in the progress of atmospheric corrosion with time of various metals (1)	17
3.	Effect of copper and surface on corrosion rate of rolled steel and malleable iron. Results obtained by Mannweiler (36)	30
4.	Front view of equipment	37
5.	Schematic diagram of equipment	38
6.	Principle of operation of the Cahn RG electrobalance	40
7.	Weight gain versus time for 4340 steel in the presence of moist air (49% R.H.). Microbalance and chamber results	56
8.	Weight gain versus time for 4340 steel in the presence of moist air (75% R.H.). Microbalance and chamber results	57
9.	Weight gain versus time for 4340 steel in the presence of moist air (98% R.H.). Microbalance and chamber results	58
10.	Corrosion rates versus time for 4340 steel in the presence of moist air (49%, 75% and 98% R.H.).  Chamber results	64
11.	Weight gain versus time for 4340 steel in the presence of dry SO <sub>2</sub> . Microbalance and chamber results	66
12.	Weight gain versus time for 4340 steel in the presence of moist SO <sub>2</sub> (49% R.H.). Microbalance and chamber results	69

Figure		Page
13.	Weight gain versus time for 4340 steel in the presence of moist SO <sub>2</sub> (98% R.H.). Microbalance and chamber results	70
14.	Weight gain versus time for 4340 steel in the presence of moist SO <sub>2</sub> (98% R.H.) (curve A), and moist air (98% R.H.) (curve B). Microbalance and chamber results	73
15.	Corrosion rates versus time for 4340 steel in the presence of moist $SO_2$ (98% R.H.) and moist $SO_2$ (49% R.H.). Chamber results	76
16.	Weight gain versus time for magnesium AZ31B in the presence of moist air (49%, 75% and 98% R.H.). Microbalance results	77
17.	Corrosion rates versus relative humidity for 4340 steel and magnesium AZ31B after 72 hours of exposure Microbalance and chamber results	83
18.	Weight gain versus time for magnesium AZ31B in the presence of dry SO <sub>2</sub> . Microbalance and chamber results	84
19.	Corrosion rates versus time for 4340 steel and magnesium AZ31B in the presence of dry SO <sub>2</sub> .  Microbalance and chamber results	87
20.	Weight gain versus time for magnesium AZ31B in the presence of moist SO <sub>2</sub> (49% R.H.). Microbalance and chamber results	88
21.	Weight gain versus time for magnesium AZ31B in the presence of moist SO <sub>2</sub> (98% R.H.). Microbalance and chamber results	89
22.	Corrosion rates versus time for magnesium AZ31B in the presence of moist SO <sub>2</sub> (49% R.H.) and moist SO <sub>2</sub> (98% R.H.). Chamber results	94
23.	Schematic diagram of the system showing the changes suggested in order to achieve better reproduction of environmental conditions in the laboratory	101

#### T. INTRODUCTION

Atmospheric corrosion of metals can be studied by means of field tests, service tests and laboratory tests. The selection of the test depends on several factors such as the environmental conditions at which the test is going to be performed, the time that can be taken in arriving at results, reliability of the test and the information that is desired.

In field tests, samples are exposed to real conditions and, hopefully, better correlation with service performance can be obtained. Field tests are carried out either at standard test sites which are typical of service atmospheres likely to be encountered and in which the environmental conditions are reasonably well known. Alternatively, field tests are conducted in service environments where the exposure conditions may be unknown. Acceleration of field tests is possible by exposing the samples adjacent to the source of the corrosive environment.

Service tests are more extensive and objective than field tests, but they are more costly and complex since the sample to be tested is placed in actual conditions of service. Normally, service tests are preceded by laboratory and field tests in order to have some initial information about the behavior of the sample under the conditions of the service test.

In laboratory tests, the performance of a metal is evaluated by simulating and/or accelerating the conditions at which it will be used. Acceleration is accomplished either by increasing the time of exposure to the critical conditions of the environment, or by intensifying the conditions of exposure such as temperature, concentration or other variables.

Among the atmospheric corrosion laboratory tests, gravimetric measurements is one of the most commonly used techniques because of its directness and general convenience. There are various forms by which these techniques can be applied.

- 1. The metal sample is weighed, placed in the corrosive atmosphere for a length of time, removed and weighed again.
- 2. The metal sample is weighed, exposed to a corrosive atmosphere and the corrosion products then are removed from the metal surface.
- 3. The metal sample can be suspended by a wire which is connected to a suitable balance, and continuous readings of the weight changes can be taken on the balance without the sample having to be removed from the corrosive atmosphere.

The last technique has the advantage that it allows the determination of the progress of corrosion products with time and, for this reason, it involves the use of a very sensitive balance (mostly microbalances) which is capable of detecting small mass changes.

For many years, the first two methods have been used widely for the determination of corrosion rates, but no information is available about the latter method in atmospheric studies. As a result of this lack of information, it is not clear whether the continuous reading technique using a microbalance is useful for laboratory tests involving corrosive atmospheres, or if this technique is sensitive enough to be reliable for atmospheric corrosion studies.

The main purpose of this study is to design, assemble and test a laboratory system based on gravimetric techniques for the determination of atmospheric corrosion rates on samples of magnesium alloy AZ31B and low alloy high strength steel 4340, and to correlate these results with literature values obtained for these materials in field tests.

The system consists of a Cahn electrobalance model RG capable of measuring changes in mass of 0.1 microgram; a potentiometric recorder to provide changes in weight with respect to time, and a gas handling system for the supply of the corrosive environments.

Sulfur dioxide and moisture in air were the atmospheres chosen for the present study, since it is well known from the literature that the synergistic effects of these two substances produce one of the most corrosive conditions that we can find on materials in field service.

Magnesium alloy AZ31B and low alloy high strength steel 4340 were selected because they are available in our laboratory, information has been gathered about atmospheric corrosion of these materials and comparisons are possible, and they are representative examples of atmospheric corrosion of a non-ferrous and a ferrous metal.

Tests have been accelerated by intensifying the conditions at which samples were exposed. For this particular study, the concentration of sulfur dioxide and relative humidity have been increased with respect to those normally encountered in field service.

The study is divided into two parts. In the first part, the environmental conditions have been simulated by using a chamber where

samples of both metals were exposed to the corrosive atmospheres and weighed after exposure. In this stage, weight losses were determined by removing the corrosion products formed on the surface of the samples. Data obtained in this first part was used to calibrate the microbalance for continuous measurements.

In the second part of the study, weight changes have been measured by means of the microbalance and corrosion rates obtained in this form were compared with the results obtained in the chamber.

#### II. ATMOSPHERIC CORROSION OF METALS

Metals are thermodynamically unstable and corrode when exposed to the atmosphere. The rate of corrosion depends on the material, moisture, dust content of air, and gaseous impurities which favor condensation of moisture on the metal surface.

Atmospheric corrosion can be divided in the following types (1, 18):

- 1. "Wet atmospheric corrosion", caused by visible droplets of condensed moisture which forms a moisture film on the surface, such as moisture resulting from dew, frost, rain, snow, etc. This corresponds to a relative humidity of 100%.
- 2. "Moist atmospheric corrosion" occurs at a relative humidity of less than 100%, and proceeds under an extremely thin, invisible film of electrolyte formed on the surface by capillary action or chemical condensation.
- 3. "Dry atmospheric corrosion" takes place in the complete absence of a moisture film on the metal surface. Dry atmospheric corrosion processes also are known as "dry oxidation" or "tarnishing" (2). An example of dry atmospheric corrosion at normal temperature is the tarnishing of copper and silver in the presence of hydrogen sulfide.

In practice is not always possible to differentiate these three forms of atmospheric corrosion, because gradual transition from one form to another is possible. For example, metals initially corroded in air by the dry corrosion mechanism can corrode by the wet mechanism

as a result of increase of moisture or formation of hygroscopic corrosion products. With direct precipitation (e.g. rain) of water the atmospheric corrosion is converted from moist to wet, but after surface drying it returns to the moist type. Thus transitions from one to another type of corrosion are possible.

Since the rate of atmospheric corrosion is related closely to the amount of surface moisture, the character of this dependence is represented by Fig. 1.

Zone I corresponds to the initial state of moisture adsorption, when thin adsorption films cannot yet be considered as continuous films possessing properties of an electrolyte. This zone refers to the minimum corrosion rate corresponding to film formation in a dry atmosphere (dry atmospheric corrosion). It is important to note that in the absence of moisture, metals exposed to the atmosphere corrode at a negligible rate (3, 4, 5).

In zone II, as a result of the phenomenon of chemical adsorption, thickening of the adsorption layer takes place, and a moisture layer is formed. The thin moist film, initially invisible, now converts to an electrolyte. At this stage, transition of the corrosion mechanism from chemical to electrochemical corresponds to a rapid increase in the corrosion rate (moist atmospheric corrosion).

In zone III, further thickening of the films of moisture will cause some lowering of the corrosion rate because of decreased oxygen diffusion through the thickened film of moisture (wet atmospheric corrosion).

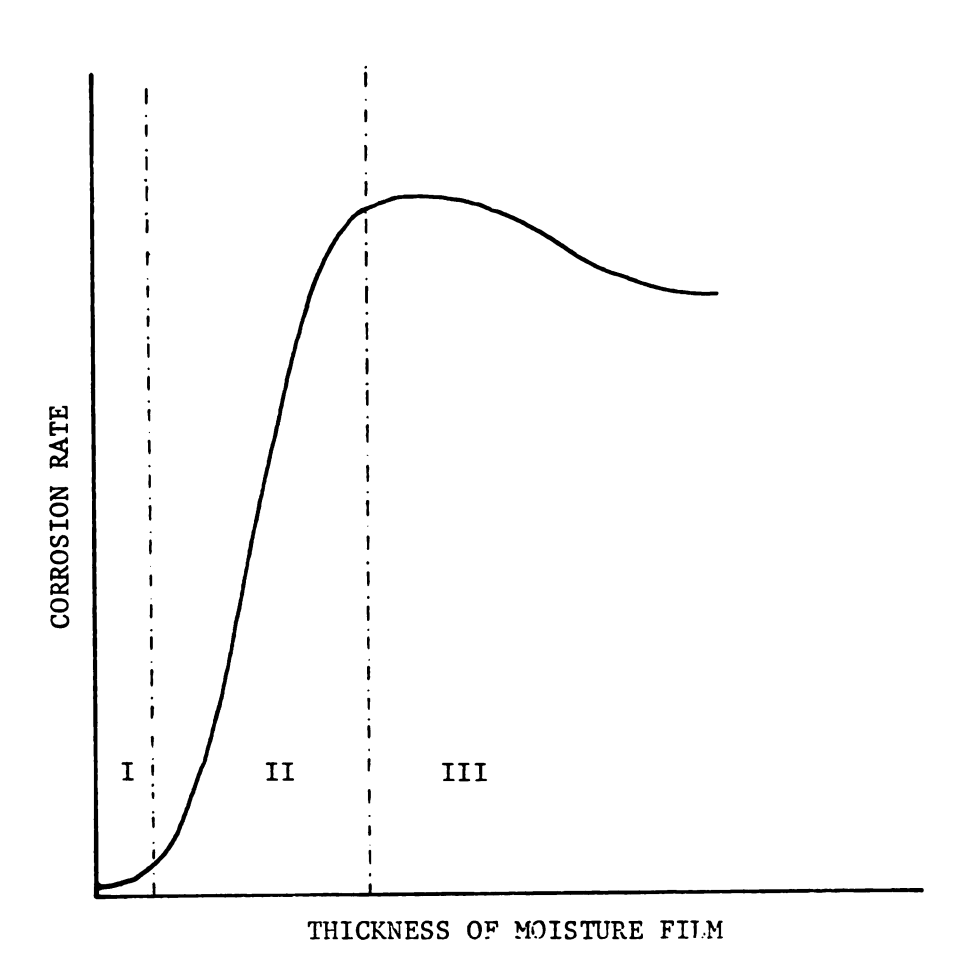


Figure 1. Dependence of atmospheric corrosion on the amount of surface moisture (1).

### A. Types of Atmospheres

Atmospheres vary greatly with respect to moisture, temperature and contaminants. Because of marked differences in corrosivity, it has been convenient to divide atmospheres into types, the most important of which are: industrial, urban, marine, tropical and rural, and there are combinations of them with large differences in corrosivity. For instance, approaching the seacost, air has increasing amounts of sea salt, in particular sodium chloride, while at industrial areas, appreciable amounts of sulfur dioxide and lesser amounts of hydrogen sulfide, ammonia, nitrogen dioxide and various suspended particulates are found. Thus a metal that resists one atmosphere may lack effective resistance in other place, and hence, relative performance of metals may change with location. In general, moist, highly contaminated industrial atmospheres are the most corrosive, whereas pure and very dry rural atmospheres are the least corrosive (1).

## B. Factors Influencing Corrosivity of the Atmosphere

The extent of atmospheric corrosion is mainly determined by (1-7):

- 1. Weather conditions
- 2. Atmospheric pollutants
- 3. Nature of corrosion products
- 1. Weather conditions. Weather parameters include relative humidity, dew point, temperature and precipitation (6). All of them affect the rate of corrosion, but those parameters related to water have the largest effects.

Vernon (8) found that an increase in the rate of corrosion will occur only beyond a "critical humidity", and that below this critical humidity the rate of corrosion is very slow.

The value of the critical humidity varies from one metal to another and also this value can change as a result of the presence of pollutants. Experimental values for the critical relative humidity for different metals are found to be between 50 and 70% when there are no other factors present, but this relative humidity is reduced to about 60% in the presence of pollutants such as sulfur dioxide.

Another significant factor in the above discussion is the percentage of the time during which the relative humidity exceeds the critical value (9). This period of time is known as "time of wetness" and it has been shown (10, 11) that it is the most important factor promoting atmospheric corrosion of metals.

As a confirmation of the last statement, Tomashov (1) cites the fact that the corrosion process develops more rapidly on the surface of the metal facing the ground than on the upper surface directly exposed to precipitation, because the period of time the moist film remains on the surface oriented towards the ground is much longer than on the upper surface because of slower drying.

A film of moisture is deposited from humid air on metal surfaces under different conditions (12); if the metal is colder than the air, if hygroscopic corrosion products or pollutant deposits are present, or through the chemisorption phenomenon.

Exposed surfaces wet immediately in the presence of dew, rain or fog. Dew condensation (4) occurs when air cools to its dew point temperature, corresponding to 100% relative humidity. The air itself needs not to cool to this point before moisture accumulates, the only requirement is that the metal surface be sufficiently cooler than the surrounding air.

Samsami and Summitt (13) studied the conditions necessary for dew to appear. They state that at night, outdoor surfaces radiate heat to the sky and become colder to the ambient air. However, an object cooler than the surrounding air absorbs heat from it because of convective flow of air over the object, so that the radiactive cooling effect is opposed by a convecting warming effect. When the warming effect is present, the object temperature drops slowly and approaches the equilibrium temperature. The authors concluded that dew appears only if the dew point is between the ambient temperature and the equilibrium temperature of the object.

Rainfall has different effects on the rate of corrosion of metals. Rain promotes corrosion by providing moisture and washing away soluble corrosion products. On the other hand, rain retards corrosion by washing away pollutant deposits. Thus, some believe (4) that heavy rain is more beneficial than light rain. Generally, however, rain probably should be considered a harmful source of moisture.

Although it remains difficult to predict the effect of temperature on corrosion processes in the atmosphere, it is thought that temperature strongly influences the rate of corrosion, since corrosion rates increase as temperature rises. Rozenfeld (14) considers the interaction of temperature and moisture, and points out that the time of wetness will vary with temperature. Thus, corrosion rates are greater at low temperatures than at warm temperatures, because moisture remains on metal surfaces longer at low temperatures but evaporates faster at warm temperatures. Tomashov (1) has a different point of view, and he showed that there is a drastic increase in corrosivity on passing from

low to higher temperatures because of an increase in the rate of the electrochemical process, when surface moisture films change from solid aggregate to a liquid state. He also found that a further increase in the pemperature produces an increased rate of corrosion activity when the increase in temperature does not cause a reduction in moisture on the metal surface by evaporation.

- 2. Atmospheric pollutants. Pollutants are substances that can cause accelerated corrosion through chemical attack or by inducing condensation. The pollutants known to contribute to atmospheric corrosion in a greater extent are described below.
- a. Sulfur and sulfur oxides are the most corrosive constituents of industrial atmospheres. They are produced from the refining of petroleum, the smelting of ores containing sulfur, the manufacture of sulfuric acid and from the burning of coal, oil and gasoline. Among sulfur oxides, sulfur dioxide is the most important of them from the corrosion viewpoint, because of its deleterious effects on many materials.

Concentrations of sulfur dioxide in urban areas ranges from 0.01 parts per million to 0.18 parts per million, however, concentration as high as 2.9 parts per million have been measured less than 1 kilometer from coal fired power plants (15).

Atmospheres polluted with sulfur dioxide have been found to be among the most corrosive of all atmospheres, and to be even more corrosive than some marine atmospheres. Under normal conditions, damage to metals and other materials by the oxides of sulfur increases with increasing relative humidity and temperature (15, 16). Preston

and Sanyal (17) found that the addition of traces of sulfur dioxide to atmospheres with relative humidity between 70 and 90% greatly increased the rate of corrosion of steels.

Sulfur dioxide is oxidized photochemically to sulfur trioxide, which combines with water to form sulfuric acid, the rate depending on sunlight, moisture, hydrocarbons, nitrogen oxides, etc.

A large part of the sulfur in the global atmosphere is produced as hydrogen sulfide by putrefaction of organic matter on land in the oceans and by volcanoes (4). Hydrogen sulfide, like sulfur dioxide, is oxidized in the air and eventually converted to sulfur dioxide, sulfuric acid and sulfate salts. At low concentrations such as 1 part in 32 million (2), hydrogen sulfide causes the tarnishing of copper and at higher concentrations it can accelerate the corrosion of steel.

b. Particulates. They include solid and liquid material in particle size from 0.1 to 100 microns (4). Dust, grit and fly ash settle to the ground quickly, whereas smaller particles remain suspended longer and can be dispersed over wide areas.

Particulates are classified as salts from sea spray dusts and soots from the incineration of agricultural wastes and burning of fuels.

Saline particles greatly increase corrosion rates for most metals (1). There is a deleterious effect between salt deposits and the atmospheric water content. Salts suffer a phase transformation from dry crystal to a solution droplet when the ambient water vapor pressure exceeds that of a saturated solution of the highest hydrate. Thus salt deposits both attract moisture to metal surfaces and provide the electrolyte solution necessary for corrosion to take place. In

general, the corrosion effect of sea salts on metals, decreases as the distance from the sea increases, (1-11).

On a weight basis, dust is the primary contaminant of many atmospheres. In contact with metallic surfaces, dust influences the corrosion rate markedly. Most industrial atmospheres carry suspended particles of carbon and carbon compounds, metal oxides, etc. These substances combined with moisture, initiate corrosion by forming galvanic or differential aereation cells; or because of their hygroscopic nature they form an electrolyte on the metal surface. Thus air free of dust cause less corrosion than air heavily contaminated with dust, especially if the dust consists of water soluble particles.

Soots and ash are adsorbent and intrinsically inert materials which may provide corrosive solutions of sulfur dioxide and other electrolytes at relative humidities even below 100 percent.

c. Nitrogen oxides. Nitrogen oxides are produced by the decay of organic matter and by internal combustion engines. In the latter case, internal combustion produces nitric oxide (NO) which oxidizes in the harmful nitrogen dioxide.

The chemical reactions occurring in the presence of nitrogen dioxide, hydrocarbons and sunlight produce an atmosphere which destroys organic materials such as paint films and protective coatings, exposing, in this manner, fresh metal to other corrosive atmospheres.

d. Other pollutants. In the analysis of atmospheric corrosion, one also should be pay attention to the participation of substances other than those mentioned above, which are harmful to metals such as hydrocarbons and ozone. Carbon dioxide is a very common pollutant but apparently it neither initiates nor accelerates corrosion of

metals (3). Vernon (8) found that the normal carbon dioxide content of air actually decreases corrosion, probably by favoring a more protective film.

3. The Nature of the corrosion products. In general corrosion products formed in atmospheric corrosion tend to be protective and act as a barrier between the atmosphere and the metal surface where the electrochemical reaction is taking place (1, 2, 3, 6).

In this case, the primary products of reaction are insoluble and protective. Typical examples are sulphate on lead, and chloride on silver. Another example where the corrosion products act as a protective barrier is in copper-bearing low alloy steels better known as "weathering steels", Wranglen (19) considers that the action of copper in reducing the atmospheric corrosion rate of iron is because of the low solubility of copper sulfide in the presence of moisture.

On the other hand, there are cases where corrosion products are not protective as the case when soluble salts are present (e.g. sodium chloride or ammonium sulfate), then the corrosion products formed under this form are soluble and readely removable, therefore the corrosion process continues unabated.

With metals such as iron, zinc and aluminum, the corrosion products consist of their insoluble hydrated oxides, formed as the result of three or four continuous processes. For iron this is expressed as:

$$Fe \rightarrow Fe^{2+} + 2e$$
 (anodic process) (1)

$$\frac{1}{2}0_2 + \text{H}_2\text{O} + 2\text{e} \rightarrow 2\text{OH}^-$$
 (cathodic process) (2)

$$Fe^{2+} + 2OH^{-} \rightarrow Fe (OH)_{2}$$
 (3)

$$2Fe(OH)_2 + H_2O + {}^{1}_{2}O_2 \rightarrow 2Fe(OH)_3$$
 (4)

The formation of corrosion products proceeds directly in the anodic regions of the metal surface. This occurs because under a thin moisture film the products of the anodic reaction (metal ions) and the cathodic reaction (OH ions) react within the electrolyte film adjacent to the metal surface.

The corrosion products formed in this way are also likely to contain chlorides and sulphates in amount dependent on the level of pollution, and these may influence the rate of corrosion.

Metal surfaces located where they become wet or retain moisture but where rain cannot wash the surface, may corrode more rapidly than metal surfaces fully exposed because of the presence of pollutants (sulfuric acid for example) adsorbed by rust in the case of iron, will continue to accelerate corrosion by means of the cycle (3):

Fe 
$$\frac{\text{H}_2\text{SO}_4^{+\frac{1}{2}\text{O}_2}}{\text{FeSO}_4}$$
 FeSO<sub>4</sub>  $\frac{\frac{1}{4}\text{O}_2 + \frac{1}{2}\text{H}_2\text{SO}_4}{\text{Fe}_2\text{Fe}_2\text{(SO}_4)_3} \frac{3/2 \text{ H}_2\text{O}}{3}$  (5)

Direct exposure of a metal to rain may therefore be beneficial compared to a partially sheltered exposure in the presence of contaminated atmospheres.

It also is important to point out that it has been found that the protective characteristic of corrosion products depends on the period of the year in which the metal is exposed to the atmosphere for the first time (3). In winter, the greater surface accumulation of combustion products (mainly sulfur compounds), produces a less protective initial corrosion product which affects the subsequent corrosion rate.

In Fig. 2 (1), it is shown that the progress of atmospheric corrosion with time varies for different metals, because of different protective properties of the corrosion products. For example, lead and aluminum form a good protective film of corrosion products and the shape of the curve degree of corrosion against time is logarithmic. For copper, tin and nickel, the protective properties are lower and give an approximate parabolic dependance of corrosion with time. Zinc initially gives a corrosion rate that diminishes with time but later proceeds at a constant value (almost linearly). This means that further growth of the layer of corrosion products does not significantly increases the protective properties. Iron has initially a low rate of corrosion during the chemical formation of the protective film and a higher rate of corrosion than for the other metals with further progress of corrosion. Only in prolonged corrosion and with the formation of a very thick layer of rust can there be observed some protective action of the corrosion products on iron.

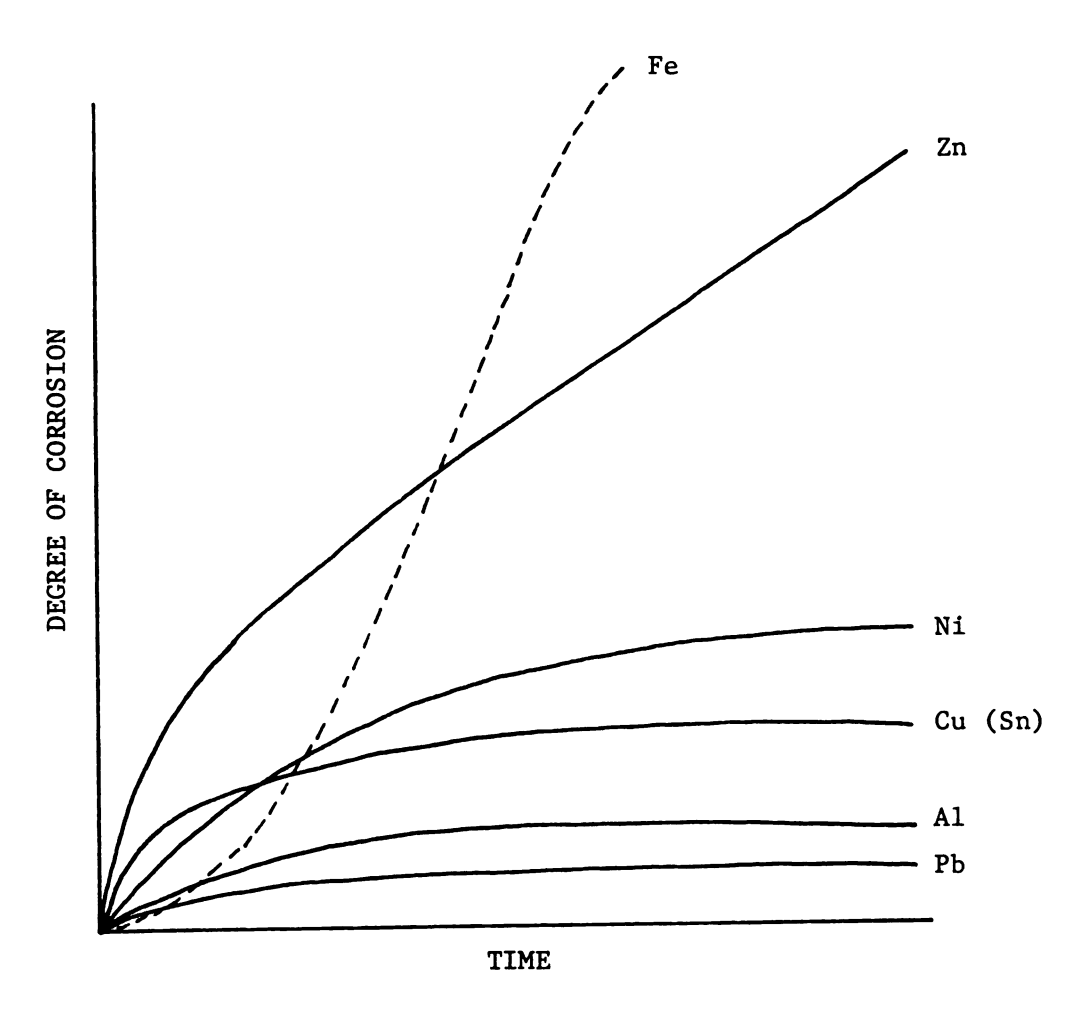


Figure 2. Effect of the protective properties of the corrosion products in the progress of atmospheric corrosion with time of various metals (1).

## III. LITERATURE REVIEW

Actually, there is no information available about the use of continuous reading techniques by means of electrobalances or microbalances in the determination of rates of corrosion caused by atmospheric corrosion; however, there are several works in which this method has proven to be successful in corrosion studies. The most important of these investigations and also other investigations not involving the use of continuous reading techniques will be discussed.

A. Atmospheric Corrosion Studies Involving the use of Continuous Reading Techniques with Microbalances.

Fryburg and Kohl (20) studied the susceptibility to hot corrosion of four nickel-base superalloys. Since the hot corrosion phenomenon depends on many factors such as temperature, composition of alloy, impurities in air and impurities in the fuel burned, the authors induced hot corrosion by coating the samples with measured doses of sodium sulfate (Na<sub>2</sub>SO<sub>4</sub>), and continuous gravimetric measurements of these samples were made at 900 and 1000 °C using a Cahn microbalance in one atmosphere of slowly flowing oxygen, with exposure times extended in some cases to over 400 hours. It was found that the order of decreasing susceptibility to hot corrosion was not in function of increasing chromium content, but in function of decreasing molybdenum content.

A similar work was carried out by Gulbransen and Meier (21). They studied the hot corrosion of simple and complex nickel-base turbine

alloys in atmospheres in coal conversion systems by means of a continuous reading microbalance, which recorded weight changes of salt-coated samples at 900-1000  $^{\rm O}$ C at 1 atmosphere pressure of slowly flowing oxygen. They found that alkali-metal contaminants in coal form low-melting sulfate salts such as sodium sulfate (Na<sub>2</sub>SO<sub>4</sub>) and potassium sulfate (K<sub>2</sub>SO<sub>4</sub>), which accelerate the corrosion rate of nickel-base turbine alloys.

Hutchings and Loretto (22) investigated the influence of composition on the oxidation of nickel-aluminum (Ni-Al) and cobaltaluminum (Co-Al) alloys. These alloys form part of a group of alloys which oxidize to produce a protective layer of alpha-alumina, the protective nature of this layer has led to the widespread use of aluminide coatings, especially in the aerospace industry. They studied the oxidation kinetics of these alloys by using a microbalance system which allowed the weight gain of the oxidizing samples to be monitored continuously to an accuracy of +2 micrograms. The microbalance output was continuously registered on a potentiometric chart recorder. The authors found that the oxidation rate of Ni-Al and Co-Al alloys is controlled by the aluminum concentration. Decreasing the aluminum concentration resulted in a reduction in the oxidation rate until the critical activity ratio, at which nickel or cobalt will be oxidized, was reached. From this point, further decreases in the aluminum concentration produced an increased oxidation rate.

Gulbransen (23) combined vacuum microbalance methods incorporating oxygen consumption with gas-flow measurements, and showed that: (a) oxide film formation, oxide volatility and transition between chemically controlled and gas diffusion controlled oxidation can be evaluated using the combined methods; (b) sample size also can be used to

evaluate the transition between chemically controlled and gas diffusion controlled oxidation; (c) gas flow can be used to extend the study of rapid oxidation reactions to rates of oxidation approaching the collision rate of oxygen with the metal surface, and (d) thermochemical analysis of the condensed and volatile oxides is very useful in the analysis of high temperature oxidation processes.

Murray (24) investigated a new technique for the study of the corrosion and oxidation of iron, involving Mössbauer spectra and microbalance data in situ at elevated temperatures, in order to obtain qualitative and quantitative information about the compounds produced. At first, he recorded the change in weight of the sample, suspending it from the arm of a microbalance by a rigid quartz fibre, at the same time as the high temperature Mössbauer spectrum. This part of the experiment failed to achieve its objective, because the fibre was found to swing and caused the Mössbauer spectrum to show considerable line broadening. Secondly, an iron foil was suspended on a jointed quartz fibre from the beam of the microbalance in a moist oxygen/sulfur dioxide atmosphere at room temperature. Although the microbalance underwent full scale deflection after two days of exposure, the author concluded that according with the quality of the spectra obtained, it is possible to obtain simultaneous Mössbauer and microbalance data for the corrosion and oxidation of iron.

Other investigators have done corrosion studies using quartz crystal microbalances which are capable of reaching sensitivities of  $10^{-8}$  gram. These microbalances are based in the piezoelectric effect in which the frecuency of a suitable oriented quartz-crystal plate depends very critically on the mass of a thin film deposited on the crystal surface.

Using this technique, Rice and Phipps (25) studied the atmospheric corrosion of cobalt in different indoor environments. They found that in humid air the corrosion rate is a sensitive function of relative humidity, the rate increasing with increased relative humidity, and they concluded that the corrosion rate of cobalt in humid air was proportional to the amount of adsorbed water. It was also performed another series of experiments on cobalt foils, to examine the corrosion rate against relative humidity at 25 °C for four different sulfur dioxide concentrations, and they found that: (a) the rate of corrosion showed clear dependence on relative humidity even in the absence of sulfur dioxide (b) at sulfur dioxide levels commonly seen in urban environments the relative humidity can profoundly influence the corrosion of cobalt, (c) a critical humidity does not exist for the sulfur dioxide-moist environment, since corrosion was measured as low as 20% relative humidity well below the critical humidities cited in the literature of 65-75% relative humidity for sulfur dioxide containing environments.

Volrabova and Vlasakova (26) verified the applicability of the quartz crystal microbalance to the study of adsorption of volatile inhibitors on copper and silver and its protective action against corrosion in humid air. The authors concluded that compared with classical microbalance techniques, the quartz crystal microbalance is more sensitive even if relatively simple equipment is used. On the other hand, they also found some limitations in the applicability of the method such as: (a) it can be used only in studies concerned with metals deposited immediately on the quartz surface by vacuum evaporation, by cathodic sputtering or electrochemically, (b) it is not possible

the use of very aggresive atmospheres since the contacts between the holder and the electrodes are soon destroyed by corrosion and the quartz crystal vibration is interrupted.

Quartz crystal microbalance techniques were used with good results by Rozenfeld and Enikeev (27) to study the effect of volatile corrosion inhibitors on water vapor adsorption of iron; by Lee and Elridge (28) to study the oxidation of air-exposed permalloy films vacuum deposited; by Lee and Siegmann (29) to establish a comparison of the mass and resistance change techniques for investigating thin film corrosion kinetics; and by Sharma (30) to study the reaction of copper and its oxides with hydrogen sulfide at various relative humidities.

It is also important to mention that Li and Rogan (31) reported the breakdown of a microbalance mechanism caused by hydrogen sulfide corrosion during studies of the mechanism of hydrogen sulfide-dolomite reaction. A baffling system was designed in order to reduce infiltration of hydrogen sulfide into the balance housing from the reaction zone, avoiding damage to the balance torque coil. The authors also considered the possibility of providing protective coatings for all parts of the microbalance that are susceptible to corrosion by hydrogen sulfide.

B. Atmospheric Corrosion Studies not Involving Continuous
Reading Techniques.

Most atmospheric corrosion studies are divided in: (1) atmospheric exposure studies at established air monitoring sites, and (2) simulated laboratory tests in which specific atmospheric conditions are reproduced as closely as possible.

In both tests, the corrosion products are removed from the metal surface of the samples after certain exposure time and rates of corrosion

obtained by determining the change in weight of the samples before and after exposure. Several studies have attempted to develop quantitative relations between corrosion and environmental parameters. The most important works will be discussed.

## 1. Outdoor Atmospheric Exposure Studies

Brandt and Adam (32) studied the atmospheric corrosion of aluminum and magnesium base alloys (including wrought magnesium alloy AZ31B) at five outdoor exposure sites, which included rural, industrial, and marine type atmospheres. Samples of these materials were exposed for periods of six months, one, three, five and ten years. They evaluated the effects of exposure by measuring the tensile strength of the exposed samples compared with that of unexposed control samples, and the percent change in tensile strength was calculated from the average tensile strength of the various exposed samples and control samples tested. Brandt and Adam found that in general wrought magnesium alloys showed a loss of tensile strength for all exposure sites but they reported the greatest losses for samples exposed at the industrial site.

Ailor (33) reported a seven year exposure test of 39 alloys of eight basic metals. The samples were exposed at a marine type atmosphere and the corrosion damage was evaluated by means of change in weight tests, tension tests, pit depth determinations and visual examinations. Among the alloys tested there were four magnesium alloys which showed the results tabulated in Table 1. From this data, it can be seen that magnesium alloy HK31A-H24 (with thorium and zirconium as main constituents) showed the best resistance against marine type atmospheric corrosion, although if compared with other metals, magnesium alloys have poor corrosion resistance in marine atmospheres.

Seven-year exposure of magnesium alloys in marine atmospheres. Results obtained by Ailor (33). Table 1.

Appearance of Sample Surfaces	gray	gray	gray	gray
Loss in Strength by Corrosion (%)	24.4	24.1	25.4	36.3
Corrosion Rate (mils/year)	0.627	0.704	0.746	0.723
Weight Change (mg/dm <sup>2</sup> )	2130	2232	2368	2290
Magnesium Alloy	HK31A-H24	HM21XA-T8	ZE10XA-H24	ZH11X1-H24

Pelensky and Jaworski (34) investigated the corrosion of dissimilar metal couples exposed in the atmosphere, in the soil and in seawater. Two of the alloys included in this study were AZ31 magnesium alloy and low alloy high strength steel 4340. The corrosion rate for magnesium alloy coupled with magnesium alloy and that of steel 4340 coupled with steel 4340 after different exposure times in a tropical atmosphere, are indicated in Table 2. The authors did not report the relative humidity of the test site, but it may be noted from Table 2 that AZ31 magnesium alloy had better corrosion resistance than steel 4340 in tropical atmospheres, at least for this particular study.

Summitt and Fink (4) reported atmospheric corrosion data for several alloys used in airframe construction, including magnesium alloy AZ31B and low alloy high strength steel 4340, exposed from four to seven years periods at different test sites. The exposure sites were established at eleven air force bases, since the principal objective of this work was to implement a program for devoloping a corrosion severity classification for each air base. The environmental conditions in each one of the air bases ranged from mild to severe. Corrosion rates obtained in three different air bases are showed in Table 3.

Pearlstein and Teitell (35) reported corrosion rates of aluminum 2024-T3 and magnesium AZ31B alloys exposed in marine, open field and rain forest (characterized by high humidity) environments in the Panama Canal Zone for periods ranging from three months to four years. The authors found that the highest corrosion rates for both alloys were observed at the marine site and the lowest in the rain site. Their results are reproduced in Table 4.

Table 2. Atmospheric exposure corrosion rates (mm/year) in marine tropical atmospheres.

Results obtained by Pelensky and Jaworski (34).	AZ31 Magnesium Alloy 4340 Steel	0.031 0.069	0.037 0.055	0.034 0.037	0.025 0.046	870 0
Results obtained by Pelensky and Jaworski (34).	Exposure Time AZ31 (months)	2	7	8	15	<b>,</b> c

Atmospheric exposure corrosion rates (mm/year) in three different air force bases. Results reported by Summitt and Fink (4). Table 3.

Location Barksdale, LA.	Exposure Time (years) 6	AZ31B Magnesium Alloy 0.0050	4340 Steel
Robins, GA.	5	0.0074	0.0058
Wright-Patterson, OH.	9	0.0107	0900.0

Corrosion rates (mm/year) for magnesium alloy AZ31B after four years exposure in the Panama Canal Zone. Results obtained by Pearlstein and Teitell (35). Table 4.

Rain Forest	0.027
Openfield	0.046
Marine	0.100

Mannweiler (36) reported the atmospheric corrosion of ferrous samples exposed for seven years to the atmospheres of different sites including rural, marine and industrial environments. The materials employed were malleable and ductile iron and rolled steel. Mannweiler found that the weight loss after seven years was approximately the same as the lost by the end of the first year for most of the samples. He attributed to the progressive accumulation of corrosion products as the main cause providing additional resistance to attack. Unalloyed steel, exhibited three to four times higher weight loss when compared with malleable and ductile iron. He also detected that: (a) malleable iron were more heavily attacked in the machined condition, whereas ductile irons averaged lower corrosion in the machined condition, (b) for all the samples the most severe attack was in the marine environment, followed by the industrial and rural sites, (c) an addition of approximately one-half percent copper to malleable iron, reduced the rate of corrosion in both machined and unmachined conditions; while copper-alloyed steel had a 43 percent lower overall rate of corrosion than the unalloyed steel after seven years. These results are illustrated in Fig. 3.

Briggs (37) carried out a similar investigation in which carbon and low alloy cast steels, some machined and other unmachined, were exposed in marine and industrial atmospheres for periods of one, three, seven and twelve years. He obtained the next results: (a) unmachined cast steel surfaces with the casting "skin" intact have no significant effect on the corrosion resistance of cast steels when compared to machined surfaces regardless of the atmospheric environment, (b) the fastest rate of corrosion takes place in the marine atmosphere with

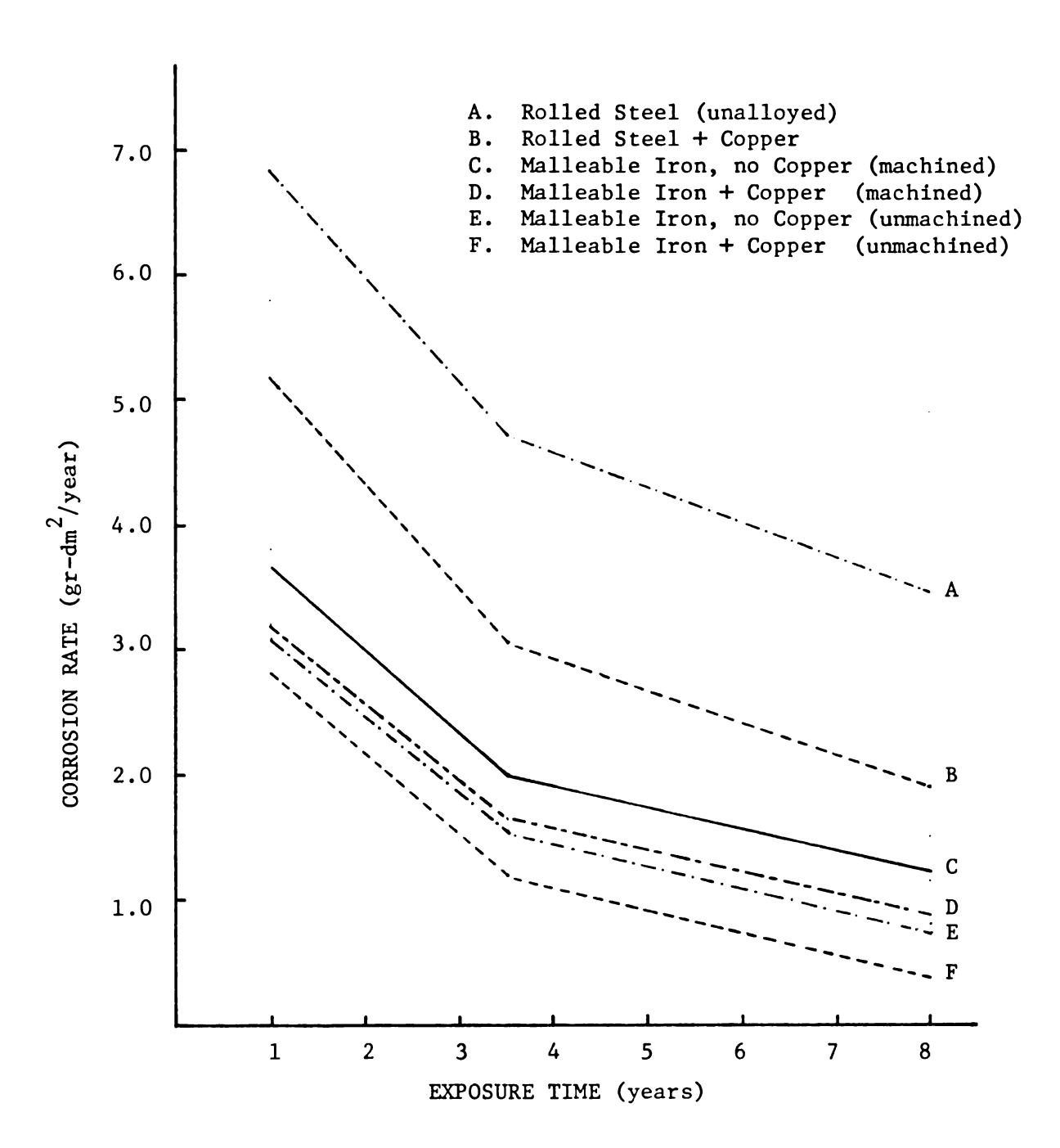


Figure 3. Effect of copper and surface on corrosion rate of rolled steel and malleable iron. Results obtained by Mannweiler (36).

lower corrosion rates occurring at the industrial atmosphere, (c) the corrosion rate of cast steel decreases as a function of time because the corrosion products act as a protective coating to the cast steel surface, (d) cast steel containing nickel, copper, or chromium as alloying elements have better corrosion resistance than carbon cast steels and those containing manganese when exposed to atmospheric environments, (e) cast steels have greater corrosion resistance than malleable iron and wrought steels in industrial atmospheres; in marine atmospheres carbon cast steel is superior to wrought steel but slightly inferior to malleable iron.

Statistical analyses also have been used extensively for determining correlation between corrosion behavior of metals and atmospheric factors.

Haynie and Upham (5) used multiple linear regression and nonlinear curve fitting techniques to analyze the relationship between corrosion behavior of a steel with low amounts of carbon and copper with atmospheric collected data. Samples of this steel were exposed at 57 different sites for a period of two years. It was found that the best empirical relationship between corrosion behavior of this particular steel and atmospheric pollution consistent with theoretical considerations, had the form:

$$corr = a_0 \sqrt{t} \left[ E^{\left( a_1 - a_2 / RH \right)} \right]$$
 (6)

where:

corr = depth of corrosion (microns)

RH = average relative humidity (percent)

a<sub>0,1,2</sub> = regression coefficients

t = time (years)

Guttman and Sereda (10) used regression analyses for determining the corrosion behavior of samples of steel, copper and zinc exposed at four inland and three coastal test sites from one to 18-month periods. They only subjected to analyses the one-month data and the equations obtained were of the form:

$$y = b_0 + b_1 A + b_2 B + b_3 C + b_{11} A^2 + b_{22} B^2 + b_{33} C^2 + b_{12} AB + b_{13} AC + b_{23} BC$$
 (7)

where:

y = corrosion loss (grams/panel)

b<sub>1</sub> = regression coefficients

A = (time of wetness, days - 14.3)/5.0

B =  $(temperature, {}^{\circ}F - 5.25)/15.0$ 

 $C = (sulfur\ dioxide,\ parts\ per\ million\ -\ 0.0202)/0.024$ 

Guttman and Sereda concluded that although the equation developed was unable to identify the atmospheric factor which exerts the most critical effect on corrosion, it indicated good correlation between the corrosion losses experienced during one-month period and the atmospheric factors.

Haynie and Upham (38) exposed samples of plain carbon steel, copperbearing steel and weathering steel to eight different industrial environments for five years. By using analyses of variance and stepwise linear regression techniques, the following equations were obtained:

Plain carbon steel

Copper-bearing steel

$$y = 8.341 [E] (4.351t)^{0.8151} - 0.00642(0X)$$
 (9)

Weathering steel

$$y = 8.876 [E]$$
 [(3.389t) 0.6695 - 0.00544(0X)] (10)

where:

y = depth of corrosion (microns)

 $SO_2$  = atmospheric concentration of sulfur dioxide (micrograms/m<sup>3</sup>)

OX = atmospheric concentration of oxidants (Ozone)  $(micrograms/m^3)$ 

t = exposure time (years).

The authors found that the effects of other pollutants such as nitrogen dioxide and nitric oxide were not significant for the corrosion of any of the steels and that more than 90% of the variability in corrosion behavior of the three types of steel can be accounted for the variability concentrations of sulfur dioxide and oxidants (primarily ozone); therefore sulfur dioxide increased corrosion and oxidants decreased corrosion. The last conclusion is supported by the fact that if corrosion rate is proportional to the accumulation of sulfates in the oxide film, an increase in the relative amount of sulfur dioxide to sulfur trioxide (SO<sub>3</sub>) instead of converted to sulfate, should reduce corrosion rate. Thus, the corrosion rate would be expected to decrease with increase in oxidant concentration (39).

#### 2. Simulated Laboratory Tests

A number of laboratory studies in atmospheric corrosion have been made in the past in order to identify the effects of atmospheric pollutants on materials. The most important works reported lately are those of Spence and Haynie (14, 40).

First, they designed a system consisting of five exposure chambers for studying the effects of gaseous air pollutants on materials. The design of the system features independent controls for regulating temperatures, relative humidities and concentrations of gaseous sulfur dioxide, nitrogen dioxide and ozone. The system also included a variable dew-light cycle that incorporates chill racks to produce dew and xenon lamps to simulate sunlight. An exposure cycle simulates night and day conditions by:

- Lamp off/dew-rack on --- moisture condenses on the test samples and adsorbs pollutants.
- 2. Lamp on/chill rack off -- moisture evaporates and pollutants react with test samples.

Dew is formed by circulating a coolant through the racks. In this manner an increase in the cycle rate yields an accelerated test.

Secondly, they used this controlled environment system to asses the direct and synergistic effects of relative humidity, sulfur dioxide, nitrogen dioxide and ozone on weathering steel and galvanized steel after 1000 hours of exposure time. The rate of corrosion was selected as the mean for assessing the effects produced by the various exposure conditions and corrosion was measured by the weight-loss method. The authors concluded that for weathering steel; sulfur dioxide, relative humidity and interaction between the two were the important corrosion rate factors, and for galvanized steel only the direct effects of sulfur dioxide and relative humidity accounted for corrosion. The empirical relationships encountered for both metals are:

Weathering steel (clean air exposure conditions)

corr = 
$$\sqrt{t_W} E^{(55.44 - 31150/RT)}$$
 (11)

Weathering steel (clean and polluted air exposure conditions)

corr = 
$$[5.64 \sqrt{SO}_2 + E^{(55.44 - 31150/RT)}] \sqrt{t_w}$$
 (12)

Galvanized steel (polluted air exposure conditions)

corr = 
$$[0.0187 \text{ so}_2 + \text{E}^{41.85 - 23240/RT}] t_w$$
 (13)

where:

corr = thickness-loss (microns)

 $t_w = time of wetness (years)$ 

R = gas constant (1.982 cal/gram - mol)

T = geometric mean temperature of panels when wet ( $^{\circ}$ K)

 $SO_2$  = concentration of sulfur dioxide (micrograms/m<sup>3</sup>).

#### IV. EXPERIMENTAL PROCEDURE

A laboratory system based on gravimetric techniques for determining atmospheric corrosion rates was designed, assembled and tested. Weight increase of magnesium alloy AZ31B and low alloy high strength steel 4340 with time was measured by means of a sensitive electromagnetic recording microbalance when exposed to different atmospheres.

Measurements were made at room temperature (20°C).

## A. Equipment

Features of the equipment consisting of: (1) Cahn electrobalance model RG, (2) control unit, (3) mass recorder, (4) gas-handling system and Mettler balance and (5) controlled atmosphere chamber are showed in Figs. 4 and 5.

A more complete description of each of the components is given below:

1. Cahn Electrobalance Model RG (41). The Cahn recording gram electrobalance (RG) is a microbalance for measuring mass and mass changes very accurately to 0.1 microgram, and provides a method of continuous measurement and recording of weight changes in the sample. The electrobalance is housed in a glass bottle which has a metal end cap with electrical feedthroughs to permit operation of the balance in controlled environments. The sample is suspended in an aluminum container by a platinum suspension wire.

# Figure 4. Front View of Equipment.

- 1. Air pressure regulator
- 2. "Drierite" tower
- 3. Flowmeters
- 4. Cahn RG electrobalance
- 5. Loop A
- 6. Loop B
- 7. Loop C
- 8. Sample tube
- 9. Sample
- 10. Counterweights
- 11. Sulfur dioxide bubbler
- 12. Sulfur dioxide drier
- 13. Moist air bubbler
- 14. To unit control and mass recorder
- 15. Gas discharge

Figure 5. Schematic Diagram of Equipment.

- 1. Air pressure regulator
- 2. "Drierite" tower
- 3. Flowmeters
- 4. Cahn RG electrobalance
- 5. Sulfur Dioxide bubbler and drier
- 6. Moist air bubbler
- 7. Gas discharge
- 8. Sample

The Cahn RG electrobalance is based on the null-balance principle, which is one of the most accurate and reliable methods of measurement. Changes in sample weight cause the aluminum beam to deflect momentarily. A flag of metal attached to the front end of the beam moves with it, causing a change in the amount of light incident on a photo-tube. The change in the photo-tube current is amplified in a servo-amplifier and the amplified current is applied to a coil attached to the beam. The coil is in a magnetic field, so current through it exerts a torque on the beam, restoring it to balance. Thus the coil current is proportional to the change in sample weight.

The beam itself is always in equilibrium since the total torque on it is zero, and the restoring torque is sufficiently powerful and fast to keep the beam locked in position even when the sample weight changes continuously. The balancing current is fed into the control unit and to a mass recorder for recording the weight as a function of time. The principle of operation is illustrated in Fig. 6.

The glass bottle enclosing the electrobalance was mounted horizon-tally on a rack. The bottle had the three downward projecting ground-glass standard-taper joints for attaching the sample tube, the glass envelope for covering suspensions from loop B and another glass envelope for covering suspensions from loop C.

Samples can be suspended either from loop A, which is designed to measure changes up to 200 mg, or loop B designed to measure weight changes up to 1 gram. Loop C is only used for counter-weights. Only loop A was used for measuring sample weight changes.

2. Control Unit. The control unit is a switch-box used for calibration and measurement of sample weight. It obtains its input from

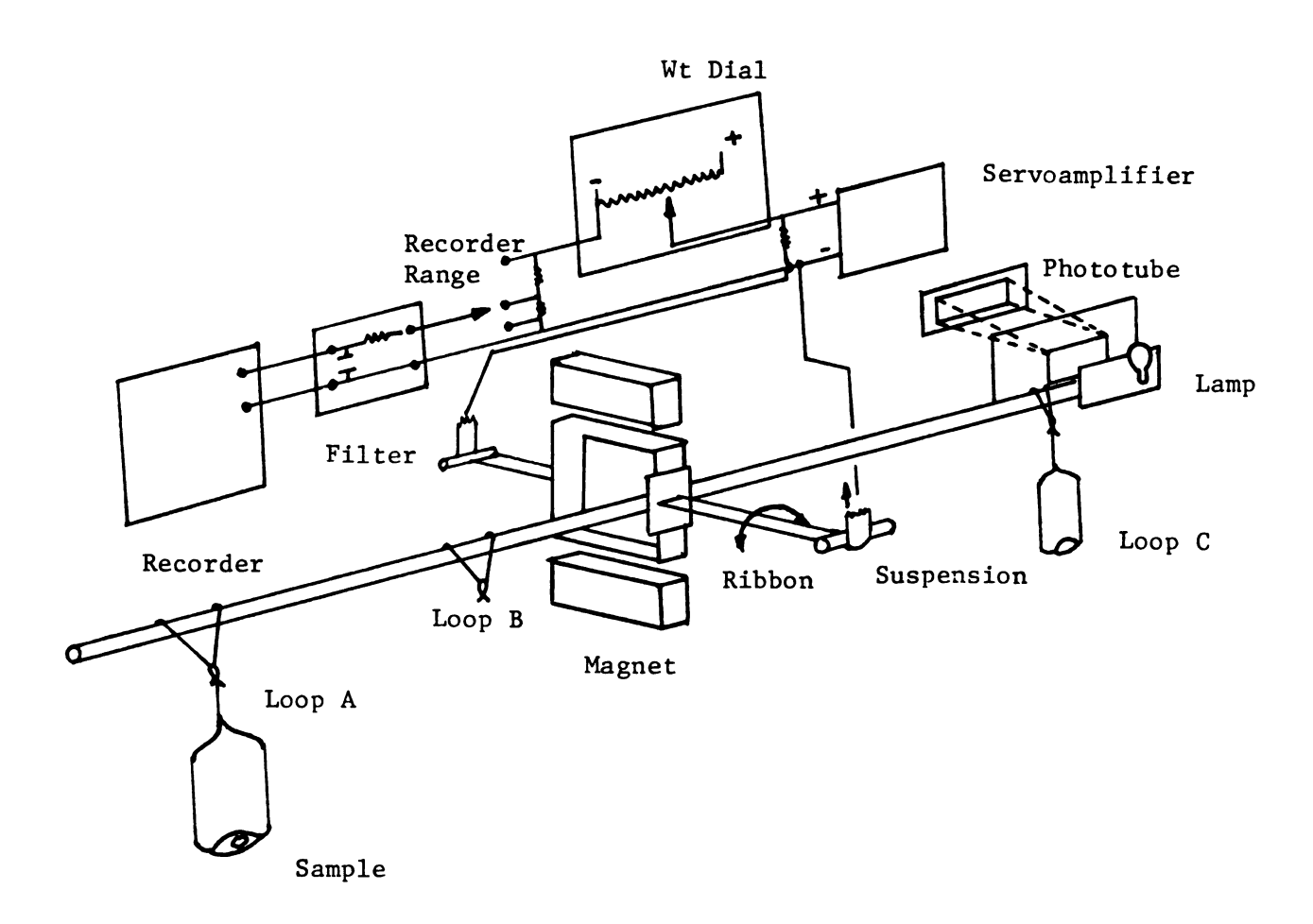


Figure 6. Principle of operation of the Cahn RG electrobalance.

the microbalance and feeds a signal to the recorder. The control unit is provided with the mass-range dial for adjusting the required change of mass to be measured, the mass dial for measuring the weight, and the recorder range dial to select the correct output to the recorder to keep the pen in the range of the chart for a maximum increase in weight.

- 3. Mass recorder. The mass recorder used in this study was a Beckman ten-inch potentiometric linear recorder, with linear spans from 0 to 1 millivolt, 0 to 10 millivolts and 0 to 100 millivolts; and chart speeds adjustable at 0.1, 0.2, 0.5, 1.0, 2.0, 5.0, and 10 inches per minute. The slower speed was used throughout the experiment.
- 4. Gas-Handling Systems and Mettler Balance. The gas-handling system was integrated by the next accesories and devices:
  - 1 Matheson flowmeter, tube number 600 with range from 8-166 cm<sup>3</sup>/min of air at 20°C and 1 atmosphere.
  - 1 Matheson flowmeter, tube number 601 with range from 8-262 cm<sup>3</sup>/min of air at 20°C and 1 atmosphere.
  - 1 Air pressure regulator.
  - 1 "Drierite" tower (CaSO<sub>4</sub>).
  - 3 Flasks of 500 ml of capacity.
  - 4 stopcocks.

Flexible plastic tubing of 6.3 cm of internal diameter.

The system was designed in such way that the next tests or combination of them could be performed:

- a) moisture in air
- b) sulfur dioxide in air
- c) combination of moisture and sulfur dioxide in air.

a) Moisture in air. Moist air at different relative humidities was produced by bubbling air through satured salt solutions in water, which give constant humidities atordinary laboratory temperatures  $(20^{\circ}C)$  (42).

Relative humidities of 49%, 75% and 98% were chosen since they represent examples of dry, mild and wet atmospheres. Details of the solubilities of the salts (43) and relative humidities obtained at different temperatures are given in Table 5.

b) Sulfur dioxide in air. Sulfur dioxide was prepared in the laboratory (44) by adding a dilute solution of hydrochloric acid (HCl), drop by drop to a solution of sodium sulfite  $(Na_2SO_3)$  according with the reaction:

$$2HC1 + Na_2SO_3 \rightarrow SO_2 + 2NaC1 + H_2O$$
 (14)

The sulfur dioxide gas liberated in this reaction was dried by bubbling it through concentrated sulfuric acid  $(H_2SO_4)$ .

c) Combination of moisture and sulfur dioxide in air. Moist ir and sulfur dioxide were combined by means of valves and stopcocks and introduced in controlled amounts into the sample tube and the test chamber. Because of the danger of damaging the weighing mechanism of the microbalance in the presence of the more corrosive sulfur dioxide atmosphere, a counterflow current of air dried with "Drierite" was used. The other function of this counterflow current was to carry the reactive gases away from the system.

A Mettler balance with capacity of 160 grams and maximum sensitivity of 0.1 milligram was used as a reference for the calibration of the microbalance and for the determination of weight losses of samples after the corrosion products were removed from the metal surface.

Saturation solubilities in water and relative humidities of lithium nitrate, sodium chloride and lead nitrate at various temperatures. Table 5.

Salt	100	150	Tempera 20 <sup>0</sup>	Temperature $(^{0}C)$ $20^{0}$ $25^{0}$	300	350	Saturation Solubility
Lithium Nitrate (LiNO <sub>3</sub> )	59	55	67	41	31	19	
Sodium Chloride (NaCl)	75	75	75	75	75	7.5	
Lead Nitrate $[Pb(NO_3)_2]$	66	86	86	6	96	96	

5. Controlled Atmosphere Chamber. A plastic chamber was built in the laboratory having dimensions of 31 cm x 21 cm x 15 cm. The chamber was used for two purposes: a) to obtain data of weight losses on samples which were used in the calibration of the microbalance, and b) to assess the reproducibility of the microbalance results by running parallel tests under the same conditions of exposure. Samples were placed inside the chamber by means of a plastic holder and glass slides.

#### B. Calibration of the Microbalance

The microbalance was calibrated by following two different procedures. In the first, recommended by the manufacturer, a little piece of wet paper was placed in loop A and the weight change due to evaporation of water from the paper was recorded. After approximately twenty minutes of recording, the trace of the recorder did not show any change in weight, so the piece of paper was removed and weighed on the Mettler balance. It was found that the weight of the dry piece of paper was in good agreement with the value obtained by the sum of the mass dial reading in the unit control plus the recorder reading. This procedure was repeated several times showing a maximum difference of 0.15 mg.

In the second procedure (45), a small grain of "Drierite" was placed in loop A and the weight gain of the sample from adsorption of atmospheric moisture was recorded. The total gain in weight after 3 hours was determined from the mass dial and recording readings and the percentage gain in weight calculated. The same procedure was followed using the Mettler balance by weighing the "Drierite" sample initially and after 3 hours. In this case the percentage increase in weight obtained with the Mettler balance showed a difference of 0.10 mg

compared with the results obtained from the microbalance, which is good considering that the maximum sensitivity of the Mettler balance is 0.1 mg.

The microbalance was calibrated to read mass changes up to 0.4 mg for a full scale deflection of the recorder pen with a maximum sensitivity of 0.0016 mg per small division of the chart.

## C. Samples

1. Samples of Low Alloy High Strength Steel 4340. Samples of low alloy high strength steel 4340, whose composition is given in Table 6, were cut from sheets which measured 12.5 cm x 14.5 cm and the final sample characterization used was 0.5 cm x 0.8 cm x 0.16 cm to give a surface area of approximately  $0.40 \text{ cm}^2$  on each side of the sample.

Twenty samples of magnesium alloy AZ31B and 4340 steel were chosen at random and their area determined. It was found that the mean area was  $0.426 \text{ cm}^2$  with a standard deviation of  $0.0275 \text{ cm}^2$  and a standard error of  $\pm 0.00616 \text{ cm}^2$ . Thus,  $0.426 \text{ cm}^2$  was the value used in further calculations for both alloys.

The size of the samples was selected taking into consideration the diameter of the container and the capacity of loop A in the microbalance.

Hardness tests and metallographic examinations were performed on five samples. Rockwell hardness tests on both sides of the samples gave an average hardness of 92  $R_b$  with maximum variations of  $\pm$  2. For the metallographic examination, samples were polished mechanically and etched as follows (46).

Chemical composition of low alloy high strength steel 4340 (%). Table 6.

	Fe	Balance
	Мо	0.20-
•(%) 0+0+	Cr	0.70-
פרוו פרפפד	Ni	1.65-2.00
e o. Chemicai composition oi iow ailoy high strength steel 4040 (%).	Si	0.20-
OW GILOY	ω	0.035 0.040
רומון מן ד	д	0.035
ii composi	Mn	0.60-
OTHERITO	ပ	0.38-
• ว		

Etching solution: Nital (7 ml of  $HNO_3$  and 100 ml of ethanol 95%)

Time of etching: 15 seconds

The surface was washed subsequently in water and dried in a stream of air.

The metallographic examination revealed a very fine structure with pearlite distributed in a matrix of ferrite (magnification 400X). This factor together with the relatively low hardness obtained, suggests that the 4340 steel sheets were normalized.

2. Samples of Magnesium Alloy AZ31B. Samples of magnesium alloy AZ31B the composition of which is given in Table 7, were cut from sheets which measured 12.5 cm x 14.5 cm. The final sample size used was also 0.5 cm x 0.8 cm x 0.16 cm with a mean area of 0.426 cm<sup>2</sup> as in the case of 4340 steel.

Hardness tests and metallographic examination were also performed on five samples. Rockwell hardness tests on one side of the samples, gave an average hardness of 11  $R_b$  with maximum variations of  $\pm$  3. Samples were polished mechanically and etched as follows (45):

Etching solution: Nital (5 ml of HNO<sub>3</sub> and 100 ml of ethanol 95%)
Time of etching: 1 minute

The surface was subsequently washed in water, then alcohol and dried in a stream of air.

The metallographic examination revealed elongated grains, caused possibly by the warm rolling process of formation of the sheets, and similar to microstructures found in reference (47). The magnification used in this case was 100x.

Table 7. Chemical composition of magnesium alloy AZ31B (%).

Mg	Balance
Zn	1.0
Si	0.10
Ni	0.005
Mn	0.20
ъ Э	0.005
nე	0.05
Ca	0.04
A1	3.0

# D. Experimental Procedure

The experimental procedure was divided in two parts. In the first part, atmospheric conditions were simulated in the chamber where samples of both metals were exposed to the corrosive environments. The main purpose of this test was to obtain information about variations in weight of the samples exposed, in order to use this information later for the calibration of the microbalance.

In the second part, once it was determined what changes in weight to expect, the microbalance was calibrated, weight changes were measured continuously and corrosion rates were obtained.

1. Chamber Test. Because corrosion rates vary at different exposure periods, planned interval tests were used. For this experiment, five intervals of exposure were selected. Thus, four samples of both metals were withdrawn from the chamber after exposure times of: 8, 16, 24, 48 and 72 hours. Although longer exposure periods can be more realistic, they were impractical for the purpose of the experiment.

The reactive gas flow introduced to the chamber was selected according to gas flows used for researchers who have already worked with the Cahn electrobalance model RG in the presence of corrosive environments, in order to assess reproducibility with the second part of the experiment. Pedersen (48) worked with a hydrogen chloride flow of 90 cm<sup>3</sup>/min and a nitrogen counterflow of 200 cm<sup>3</sup>/min for protecting the weighing mechanism of the microbalance. The author reported satisfactory results in using the latter values for a reactive gas flow and a non-reactive gas counterflow respectively. Thus, for the chamber test and for the microbalance test, a reactive gas flow of 90 cm<sup>3</sup>/min and a non-reactive gas counterflow of 200 cm<sup>3</sup>/min were used throughout the study.

The chamber test was performed following the next steps:

a) Samples of magnesium alloy AZ31B and steel 4340 were chemically cleaned prior to exposure, in order to remove oxides already formed, particles of dust, and other products from the metal surface. The standard method G-1 recommended by the American Society for Testing and Materials (ASTM) (49) was used for the chemical cleaning of the samples. For 4340 steel the following solution was used:

500 ml of concentrated hydrochloric acid (HCl)

50 gr/l of stannous chloride  $(SnCl_3)$ 

20 gr/l of antimonous chloride (SbCl<sub>3</sub>)

time of cleaning: 25 minutes

temperature of cleaning: room temperature (20°C)

the samples were subsequently washed in water and dried in a stream of air.

For magnesium alloy AZ31B the following solution was used:

500 ml of water

150 gr/l of silver chromate  $(Ag_2Cr0_4)$ 

time of cleaning: 1 minute

temperature of cleaning: boiling

the samples were subsequently washed in water and dried in a stream of air.

After the cleaning procedure the samples were weighed before exposure.

b) Samples of both metals were exposed first to moist air with a relative humidity of 75%. This relative humidity was achieved by bubbling air through a satured solution of 300 ml of sodium chloride in water. Secondly, the samples were exposed to dry sulfur dioxide which was prepared in the laboratory by adding 10 ml of hydrochloric

acid each 24 hours drop by drop to a solution of 200 ml of sodium sulfite in water according with Equation (14). The sulfur dioxide gas liberated in this reaction was dried by bubbling it through 100 ml of concentrated sulfuric acid. Finally the samples were exposed to an atmosphere containing moist air and sulfur dioxide combined.

The samples were located inside the chamber in such way that the stream of reactive gases was able to reach one side of the samples in a uniform manner during all the exposure time.

c) The samples were withdrawn after exposure periods of 8, 16, 24, 48 and 72 hours; and weighed in order to determine if there was an increase in weight because of the formation of corrosion products. After this, the corrosion products were removed from the metal surface by the same chemical cleaning procedure used before exposure and the samples were reweighed. Weight losses were obtained by substracting the weight of the sample after exposure and after cleaning from the weight of the sample after cleaning before exposure. Since the test was performed using sets of four samples; the weight loss after certain interval of exposure was taken as the average of the four samples.

In using this method, although the corrosion products are completely removed, some loss of underlying metal cannot be avoided (50). For this reason it is recommended to obtain an appropriate correction factor after the removal of corrosion products. Thus, the effect of cleaning on the samples was determined for both, magnesium alloy AZ31B and 4340 steel by:

- 1) weighing a set of 4 samples after exposure before cleaning
- 2) removing the corrosion products by cleaning after exposure

- weighing the samples after cleaning (corrosion products have been removed)
- 4) cleaning the samples again
- 5) reweighing the samples for assessing the amount of metal lost because of the cleaning procedure.

Steps 4 and 5 were repeated four times and it was found that for magnesium alloy AZ31B there was no significative lost of metal during the cleaning procedure. On the other hand, it was found that for 4340 steel there was an average lost of metal of 0.1 milligram due to the cleaning procedure. This lost of metal was considered in further calculations involving 4340 steel.

2. Microbalance Test. Once the variations in weight of the samples exposed to three different environments were determined, the microbalance was set up with the empty sample container suspended from loop A, and placing a substitution weight representing the sample weight in the container. This load was then counterbalanced as close as possible on loop C. Accurate calibration of all dials was achieved by adding and removing calibrating weights and adjusting potentiometers in the unit control. The substitution weight then was removed, and the sample placed in the container. The total sample weight was always the sum of the substitution weight, the reading of the mass dial in the unit control and the recorder reading in milligrams.

The microbalance test was performed according with the next steps:

a) In addition to the sample being tested in the microbalance, four samples of the same material were also located inside the chamber in such way that parallel tests were ran together under exactly the same conditions of exposure. The purpose of this parallel test was

to assess reproducibility of results from both the microbalance and the chamber.

- b) The samples were cleaned and weighed before exposure, following the standard method G-l recommended by the ASTM described already in the chamber test.
  - c) Samples of both metals were exposed to:
  - (1) moist air containing relative humidities of 49%, 75% and 98% by bubbling air through flasks containing 300 ml of saturated salt solutions in water. The salts used for accomplishing these relative humidities at room temperature (20°C) were:

lithium nitrate for 49% relative humidity sodium chloride for 75% relative humidity lead nitrate for 98% relative humidity

- (2) dry sulfur dioxide prepared in the laboratory according with the reaction expressed by Equation (14).
- (3) an atmosphere containing moist air at relative humidities of 49%, 75% or 98% combined with sulfur dioxide.
- d) The samples exposed in the chamber were withdrawn after exposure times of 8, 16, 24, 48 and 72 hours and weighed in the Mettler balance for determining the weight gain. The sample tested in the microbalance was not withdrawn until the end of the test; that is 72 hours. The weight gains for this sample after 8, 16, 24 and 48 hours were obtained from the recorder reading, whereas the weight gain after 72 hours of exposure was obtained from the recording reading and in the Mettler balance.

Afterwards, all samples were chemically cleaned in order to remove the corrosion products and weight losses were obtained by substracting the weight of the sample after exposure and after cleaning (final condition) from the weight of the sample after cleaning before exposure (initial condition). Correction factors as a result of lost of metal during the cleaning procedure were applied.

e) Once the weight losses were obtained in both metals for all the conditions of exposure, corrosion rates were calculated by means of the next relationship (49):

Corrosion Rate = 
$$(K \times W) / (A \times T \times D)$$
 (15)

where:

K = constant for obtaining corrosion rates in mm/year (8.76 x  $10^4$ )

W = mass loss in grams, to the nearest 1 mg

 $A = area in cm^2$ , to the nearest 0.01 cm<sup>2</sup>

T = time of exposure in hours, to the nearest 0.01 hour

D = density of the material in gr/cm<sup>3</sup>

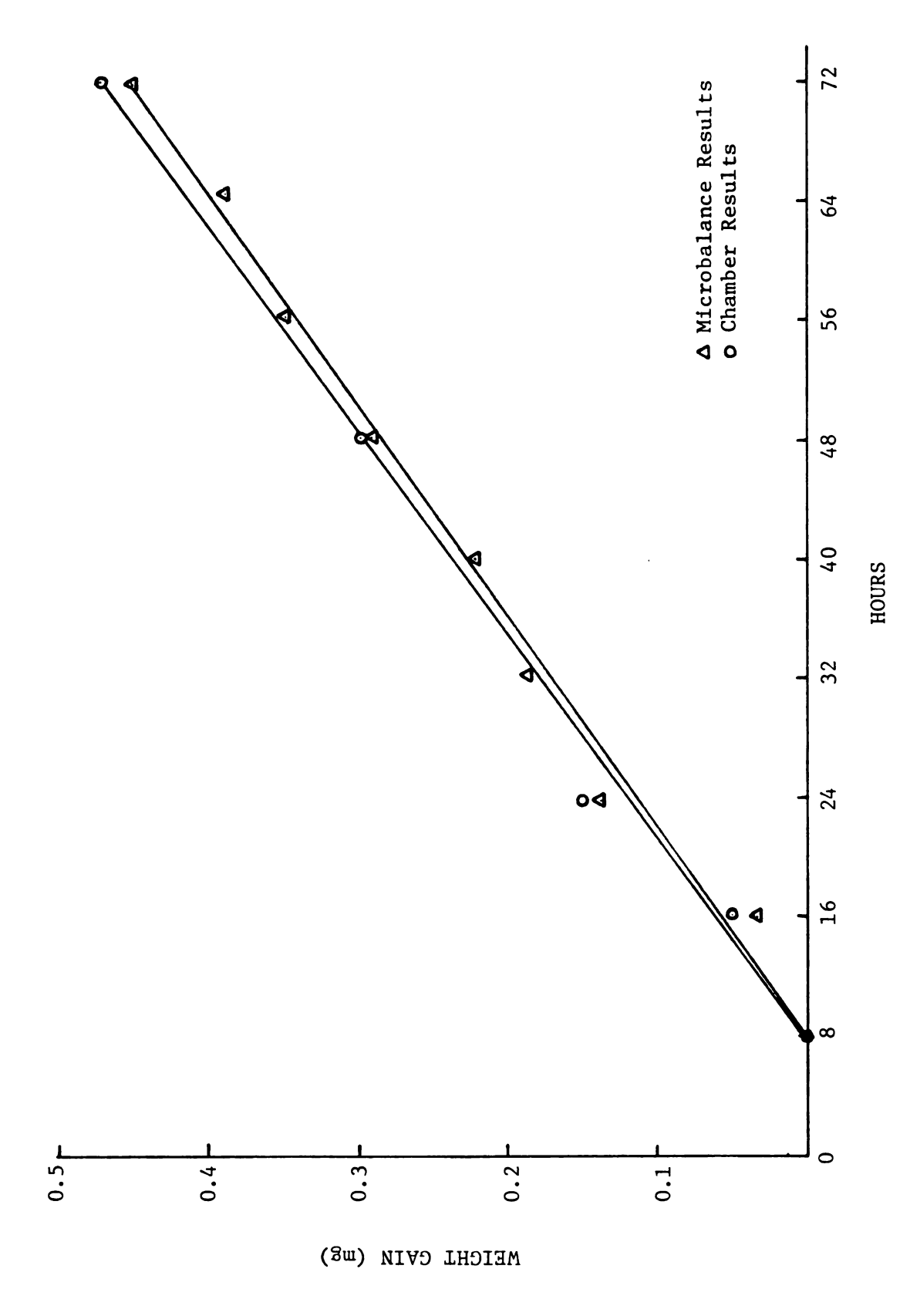
(1.74 gr/cm<sup>3</sup> for magnesium alloy AZ31B)

 $(7.85 \text{ gr/cm}^3 \text{ for low alloy high strength steel } 4340)$ 

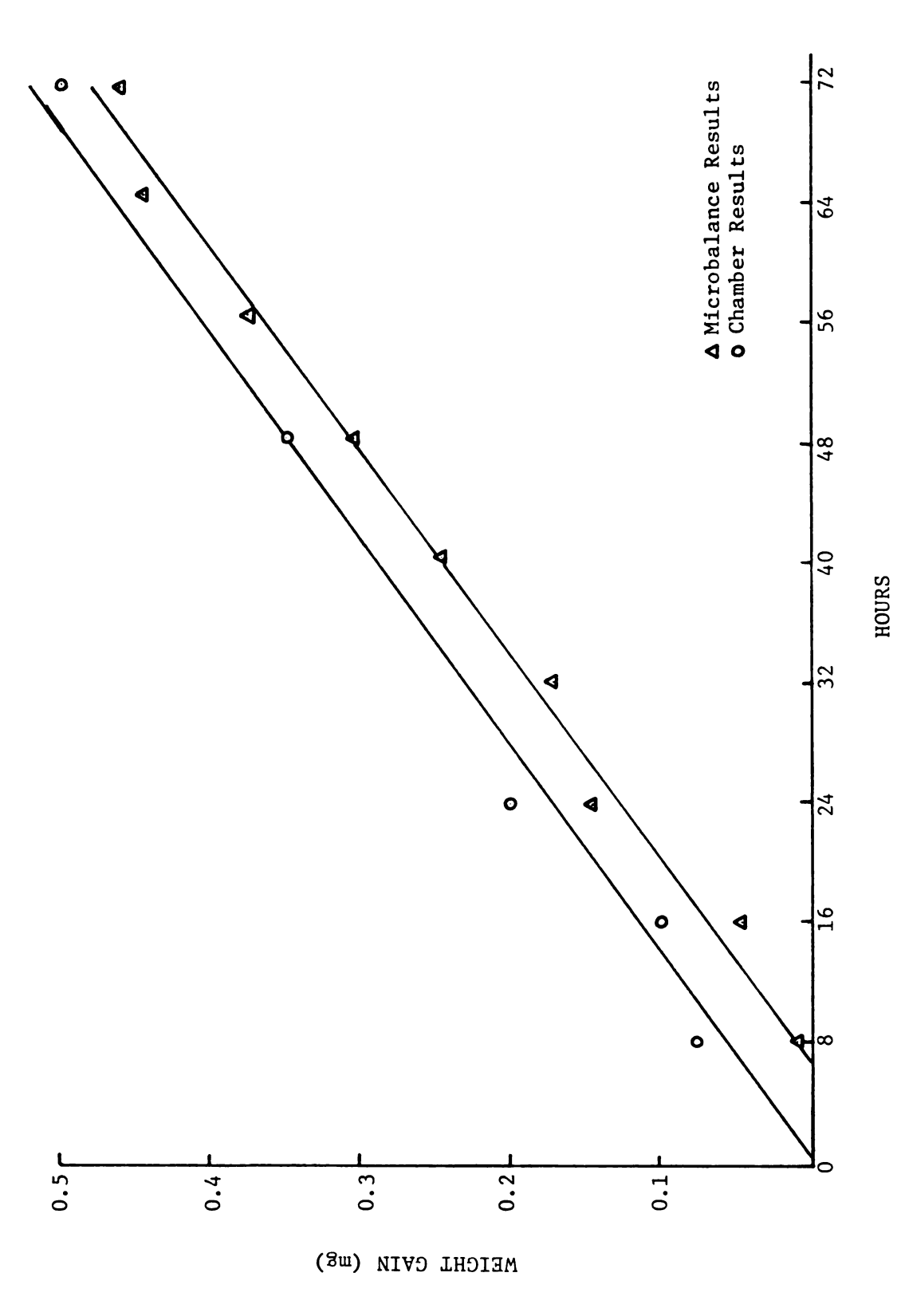
#### V. RESULTS AND DISCUSSION

# A. Low Alloy High Strength Steel 4340

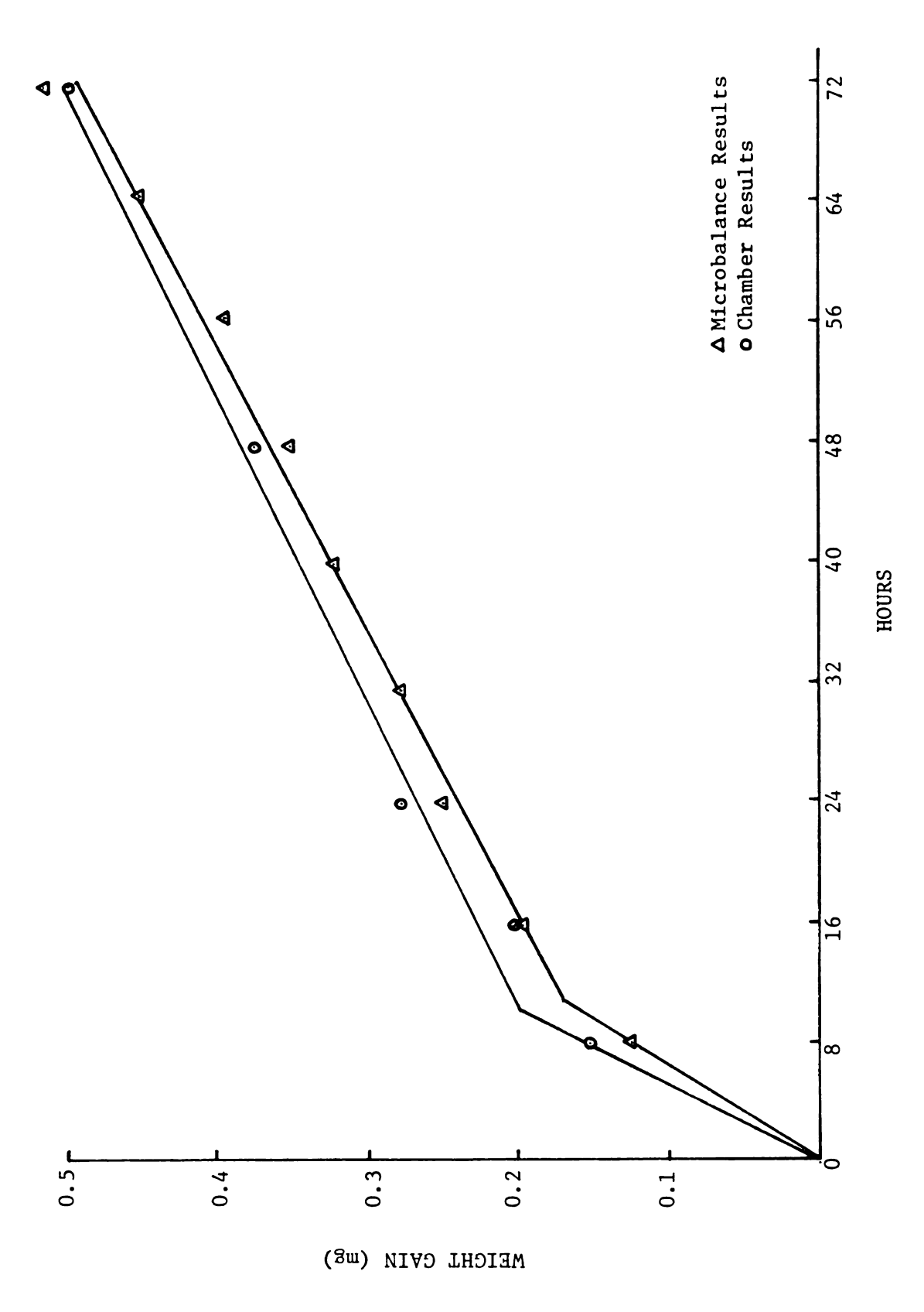
1. Moist Air Tests. Shown in Figs. 7, 8, and 9 are weight gains versus time for 4340 steel in moist air at 49%, 75% and 98% relative humidity obtained from both microbalance and chamber tests. In Tables 8, 9 and 10 are listed the values of weight gain, weight loss, and corrosion rate for 4340 steel in moist air at 49%, 75% and 98% relative humidity obtained from both microbalance and chamber tests. From the figures it is observed that at 49% relative humidity 4340 steel shows an eight-hour induction period when no weight gain was recorded in either the microbalance test or the chamber test. At 75% relative humidity this induction period decreased considerably in the chamber test but the decrease was small in the microbalance. On the other hand, at 98% relative humidity there was no such induction period and samples of 4340 steel exposed under these conditions showed a weight gain from the beginning of testing for the microbalance and the chamber. Samples removed after 72 hours of exposure presented a light formation of rust on the surface at 45% relative humidity, but at 75% and 98% relative humidity samples were totally covered by a film of dark rust. We can see also from Tables 8, 9 and 10 that after 72 hours of exposure the values of weight gain, weight loss and corrosion rate are a function of the relative humidity, that is, as the relative humidity was increased, the values of weight gain, weight loss and corrosion rate also increased.



Weight gain versus time for 4340 steel in the presence of moist air (49% R.H.). Microbalance and chamber results. Figure 7.



Weight gain versus time for 4340 steel in the presence of moist air (75% R.H.). Microbalance and chamber results. Figure 8.



Weight gain versus time for 4340 steel in the presence of moist air (98% R.H.). Microbalance and chamber results. Figure 9.

Values of weight gains, weight losses and corrosion rates for steel 4340 in the presence of moist air (49% R.H.). Microbalance and chamber results. Table 8.

	CHAM	CHAMBER (4 samples)		MICROB/	MICROBALANCE (1 sample)	(a.
Time (hours)	Weight Gain (mg)	Weight Loss (mg)	Corrosion Rate (mm/year)	Weight Gain (mg)	Weight Loss (mg)	Corrosion Rate (mm/year)
∞	0.0	0.0	0.0	0.0044		
16	0.05	0.125	0.204	0.0320		
24	0.150	0.175	0.191	0.1400		
32				0.1880		
07				0.2300		
87	0.300	0.300	0.163	0.2960		
99				0.3440		
79				0.3920		
72	0.475	0.400	0.145	0.4480	0.441	0.160

Values of weight gains, weight losses and corrosion rates for steel 4340 in the presence of moist-air (75% R.H.). Microbalance and chamber results. Table 9.

MICROBALANCE (1 sample)	Corrosion Rate Weight Gain Weight Loss Corrosion Rate (mm/year) (mg) (mg) (mm/year)	0.327 0.012	0.286 0.044	0.218 0.148	0.172	0.244	0.191 0.304	0.376	0.436	0.181 0.456 0.515 0.187
CHAMBER (4 samples)	Weight Loss Cor (mg)	0.100	0.175	0.200			0.350			0.500
СНАМ	Weight Gain (mg)	0.075	0.100	0.200			0.350			0.500
	Time (hours)	œ	16	24	32	07	87	56	99	72

Values of weight gains, weight losses and corrosion rates for steel 4340 in the presence of moist-air (98% R.H.). Microbalance and chamber results. Table 10.

ımple)	Corrosion Rate (mm/year)									0.264
MICROBALANCE (1 sample)	Weight Loss (mg)									0.728
MICI	Weight Gain (mg)	0.120	0.204	0.258	0.286	0.318	0.344	0.392	0.456	0.516
(s:	Corrosion Rate (mm/year)	0.491	0.327	0.300			0.272			0.254
CHAMBER (4 samples)	Weight Loss (mg)	0.150	0.200	0.275			0.500			0.700
CH7	Weight Gain (mg)	0.150	0.200	0.275			0.375			0.500
	Time (hours)	æ	16	24	32	40	48	26	99	72

Although it is known from the literature (6, 8, 51, 52) that the critical relative humidity for ferrous alloys is about 70%, it seems, from these results, that the critical relative humidity was attained at some point between 75% and 98% relative humidity since: a) the difference between the corrosion rates obtained at 98% and 75% relative humidity are greater than the difference between the corrosion rates obtained at 75% and 49% relative humidity after 72 hours of exposure, and b) the presence of induction periods with no weight gain at a relative humidity as high as 75%.

These results are in agreement with Vernon (52) who defines two critical humidities for steel. A "primary" critical humidity value of 50% to 65% relative humidity at which breakdown of the air-formed film occurs and attack on the metal begins, the surface becoming covered with a very fine "rust", and a "secondary" critical humidity in which a large increase in corrosion occurs with the formation of red rust.

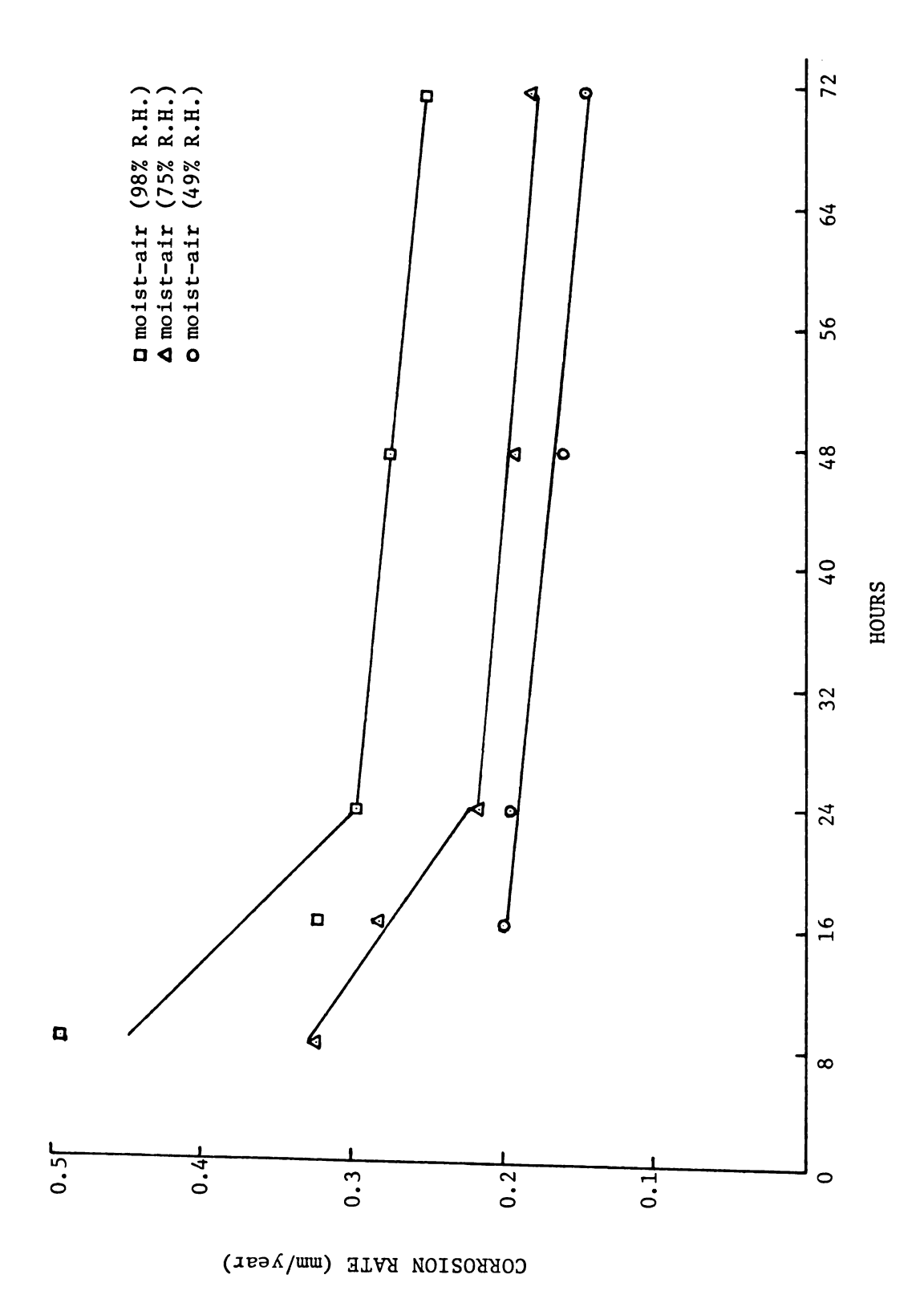
From Figs. 7, 8, and 9 it is also important to discuss the shape of the weight gain-time curves. At 49% and 75% relative humidity the curves have a rectilinear behavior which means that the film of corrosion products formed on the surface of the metal is not thick enough to decrease the diffusion of the reactants through it (52), therefore the corrosion process continues unabated under these conditions. At 98% relative humidity the film of corrosion products is thicker causing an increase in the resistance to difussion of the reactants. This means that even at prolonged exposure at this relative humidity the film of corrosion products will not grow considerably, since any thickening can take place only by diffusion of the reactants (52, 53, 54).

The shape of the curve in Fig. 9 consists of two parts. In the first part of the curve (8 hours of exposure) the growing rate of corrosion products is greater than in the second part (after 8 hours of exposure) which means that once the film of corrosion products has reached a certain thickness, further thickening proceeds slowly. Thus, according to these results, it is obvious that the film of corrosion products formed at a relative humidity of 98% is more protective against further corrosion than the films of corrosion products formed at 49% and 75% relative humidity.

According to Tomashov (1), the form of corrosion observed in moist air at 49%, 75% and 98% relative humidity is a type of moist atmospheric corrosion since the relative humidity is less than 100%. During this process a film of moisture appears on the corroding surface resulting from condensation of water, with transition from a pure chemical mechanism of corrosion to a more intensive electrochemical mechanism.

Tomashov states that condensation of moisture on the metal surface can proceed by three different mechanisms: a) capillary condensation (e.g. in crevices, dust particles in the metal surface, pores in the film of corrosion products), b) adsorption condensation produced by forces of attraction between water molecules and a solid surface. and c) chemical condensation produced by further development of adsorption condensation in the form of a chemical reaction with water and the material on which condensation takes place.

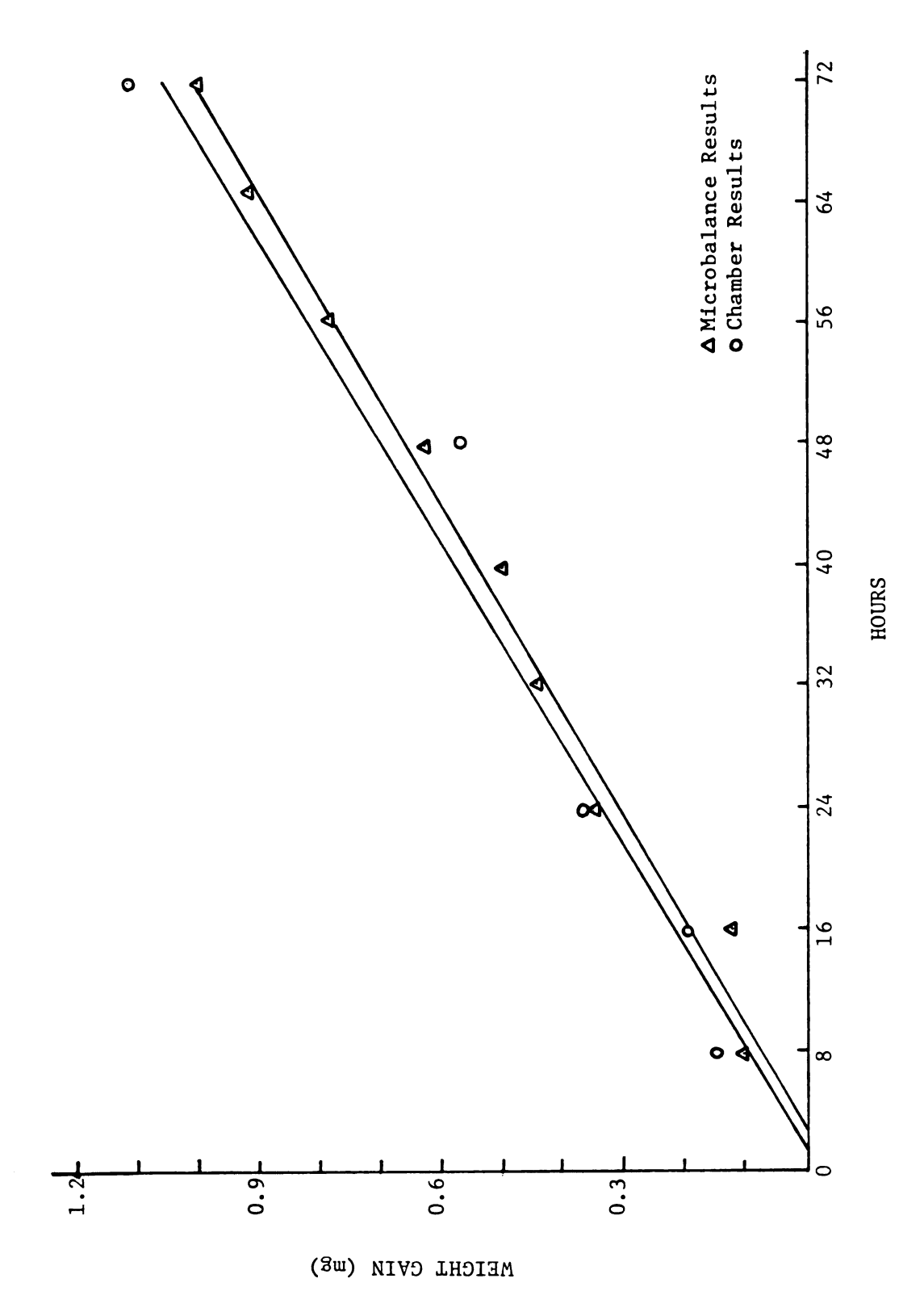
Fig. 10 shows corrosion rates versus time for 4340 steel in moist air at 49%, 75% and 98% relative humidity obtained from chamber tests. As can be observed, the corrosion rates decrease with time which means that the film of corrosion products formed on the metallic surface becomes more protective as the length of exposure increases.



Corrosion rates versus time for 4340 steel in the presence of moist air (49%, 75% and 98% R.H.). Chamber results. Figure 10.

Laboratory investigations in the rusting of low alloy steels using radioactive tracer methods (17), suggest that the number of anodic sites present in the film of corrosion products decreases drastically with time, until a point where practically no anodic sites are present is reached, providing the fact that the film of corrosion products becomes continuous and protective. This situation occurs after approximately four years of exposure.

2. Dry  $\mathrm{SO}_2$  Tests. Fig. 11 shows weight gain versus time for 4340 steel in the presence of dry  $\mathrm{SO}_{2}$  obtained from both microbalance and chamber tests; whereas Table 11 shows the values of weight gain, weight loss and corrosion rate. From Fig. 11 it also is observed that, as in the case of moist air at 49% and 75% relative humidity, there is an induction period in the first four hours of exposure when no weight gain was detected. After 16 hours of exposure, the results were comparable with those obtained in the moist air test at 98% relative humidity, but after 24 horus of exposure, weight gain started to increase rapidly and at the end of the test the weight gain was more thantwice that obtained in the moist air test at 98% relative humidity for both the microbalance and chamber tests. could be explained by the fact that although the samples were exposed just to dry sulfur dioxide, it is probable that humidity present in the laboratory interacted with the gaseous sulfur dioxide, promoting the formation of a film of moisture thus causing the high values of weight gain and corrosion rates obtained after 16 hours of exposure. Vernon (54) found that sulfur dioxide in dry air has practically no effect on the corrosion rate of steel.



Weight gain versus time for 4340 steel in the presence of dry  $\mathrm{SO}_2$ . Microbalance and chamber results. Figure 11.

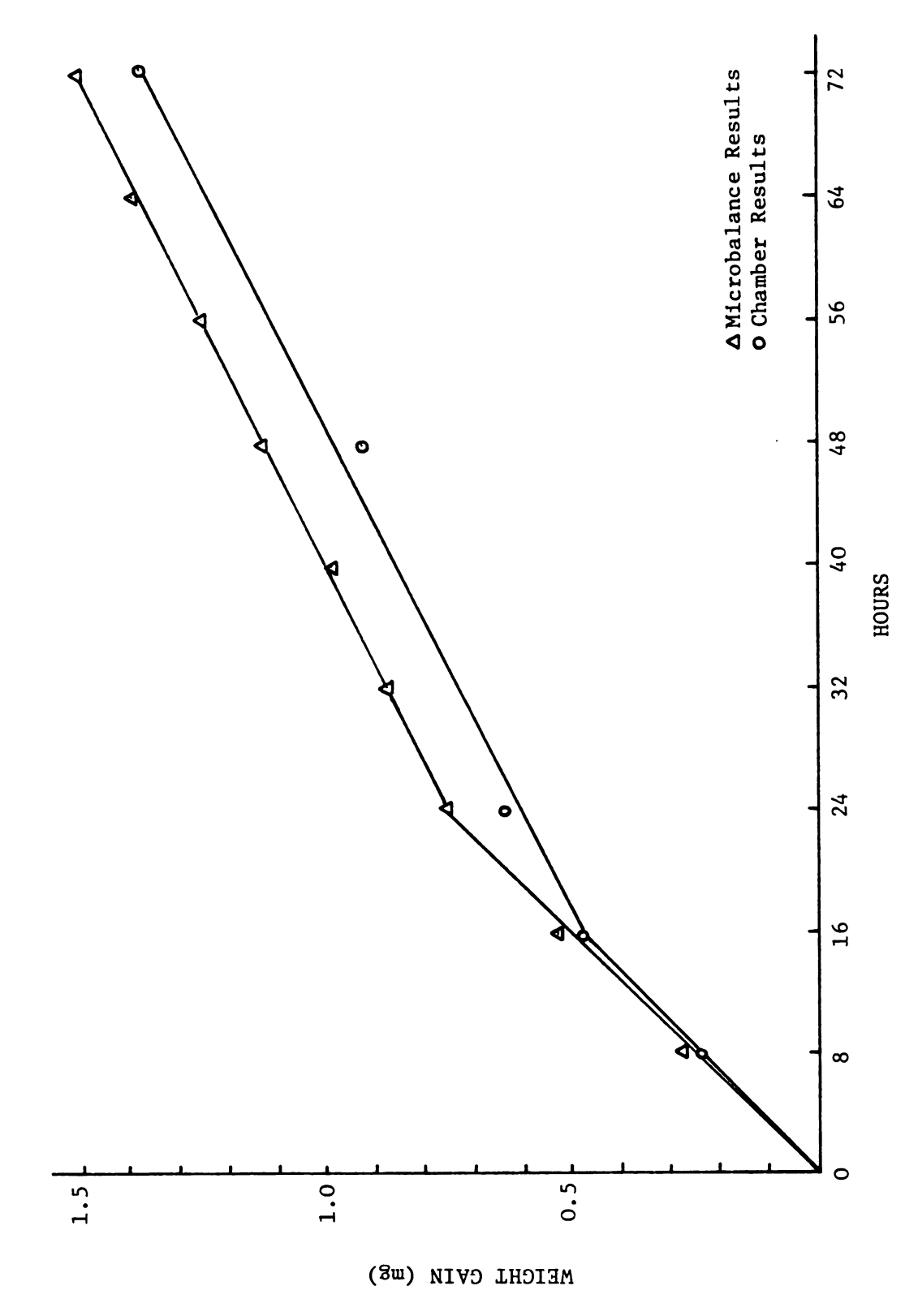
Values of weight gains, weight losses and corrosion rates for steel 4340 in the presence of  ${\rm dry-S0}_2$ . Microbalance and chamber results. Table 11.

ımple)	Corrosion Rate (mm/year)									0.354
MICROBALANCE (1 sample)	Weight Loss (mg)									0.975
MIC	Weight Gain (mg)	0.108	0.124	0.360	0.452	0.504	0.648	0.788	0.914	1.016
(s)	Corrosion Rate (mm/year)	0.654	0.450	0.436			0.382			0.363
CHAMBER (4 samples)	Weight Loss (mg)	0.200	0.275	0.400			0.700			1.000
CH7	Weight Gain (mg)	0.150	0.200	0.375			0.575			1.125
	Time (hours)	œ	16	24	32	07	87	99	94	72

3. Moist  $\mathrm{SO}_2$  Tests. Figs. 12 and 13 show weight gain versus time for 4340 steel in the presence of moist  $\mathrm{SO}_2$  at 49% and 98% relative humidity obtained from both microbalance and chamber tests. Tables 12 and 13 show the values of weight gain, weight loss, and corrosion rate for 4340 steel in the presence of moist  $\mathrm{SO}_2$  at 49% and 98% relative humidity respectively obtained from both microbalance and chamber tests. It can be observed that the presence of sulfur dioxide greatly increases the weight gain and consequently the corrosion rates in 4340 steel. The critical relative humidity that was found to be between 75% and 98% relative humidity in the moist air tests, was brought down to a value even less than 45% relative humidity in the presence of sulfur dioxide since the results of weight gain and corrosion rate obtained in the moist  $\mathrm{SO}_2$  test at 49% relative humidity were in general more than double the results obtained in the moist air test at 98% relative humidity.

These observations can be explained better from Fig. 14, where weight gain is plotted versus time. Curve A represents samples exposed to moist air at 98% relative humidity in the presence of sulfur dioxide whereas curve B represents samples exposed to moist air at 98% relative humidity without sulfur dioxide. These results are in agreement with those obtained by Taylor (17) who studied the influence of sulfur dioxide in the atmospheric corrosion produced by moist air.

It has been established (17) that the corrosion of iron in the presence of moist air containing sulfur dioxide may follow two mechanisms: The "acid regeneration cycle" and the "electrochemical cycle". In the acid regeneration cycle, sulfur dioxide and moisture are adsorbed and sulfur dioxide is oxidazed by atmospheric oxygen to



Weight gain versus time for 4340 steel in the presence of moist SO<sub>2</sub> (49% R.H.). Microbalance and chamber results. Figure 12.

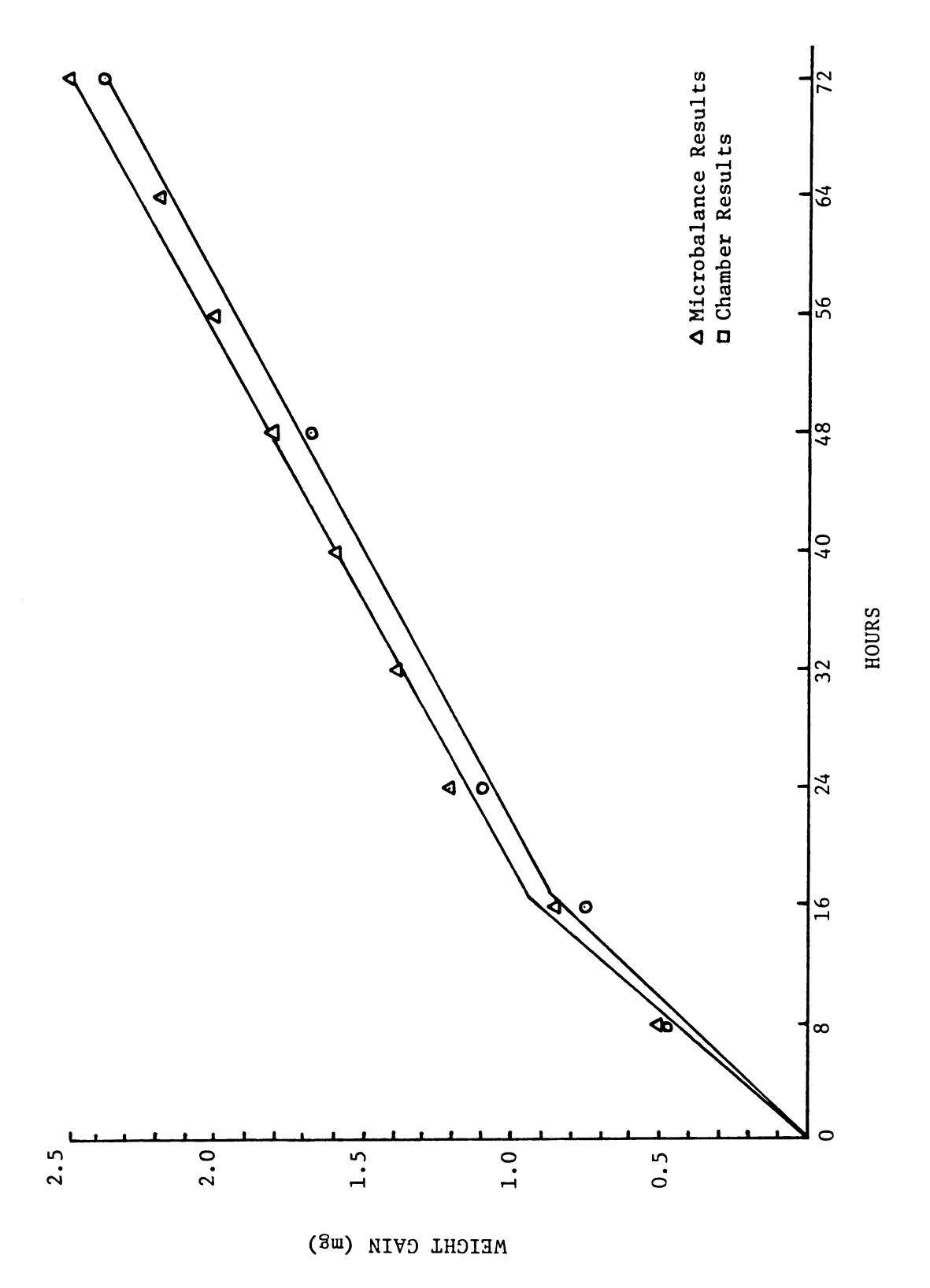


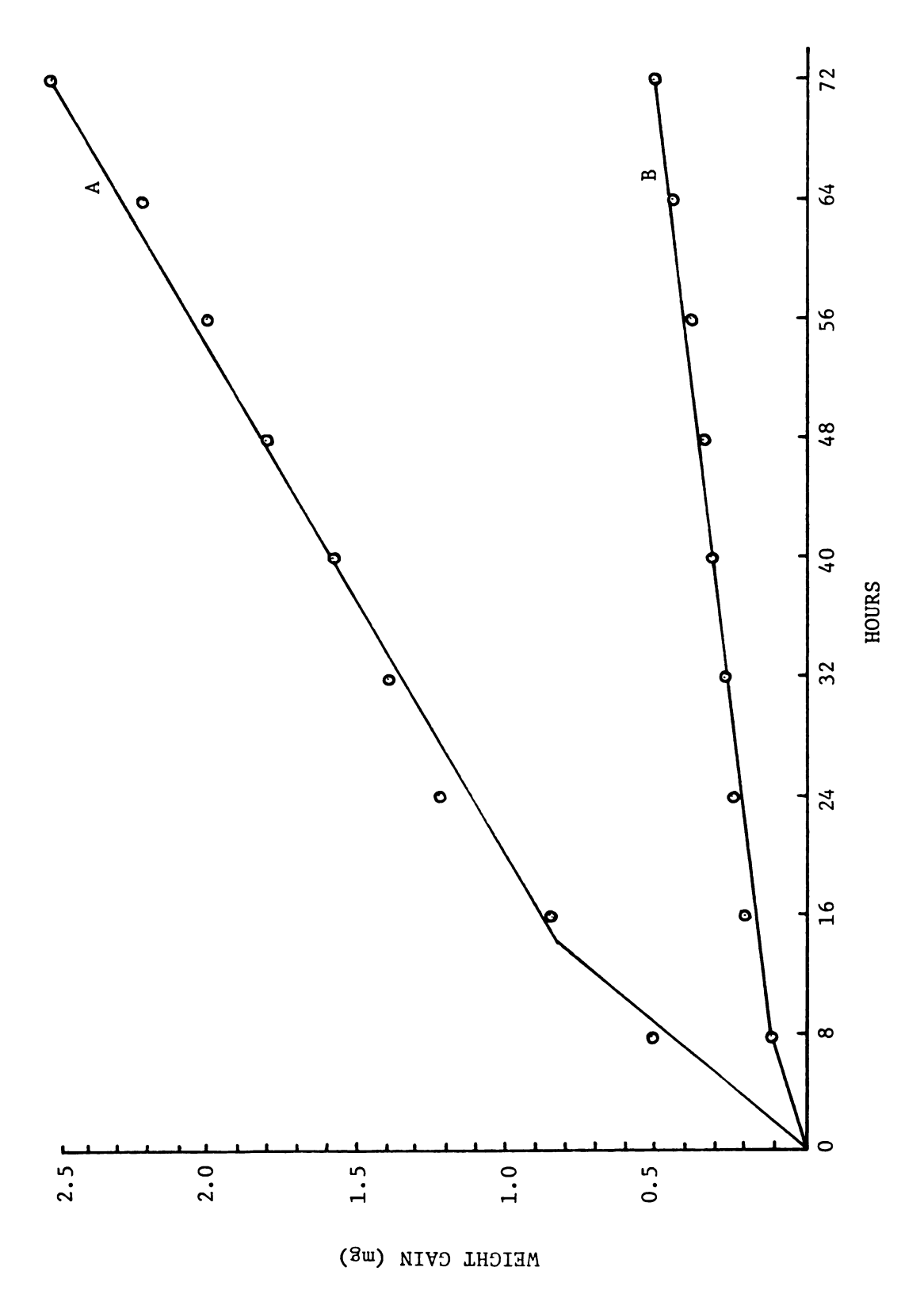
Figure 13. Weight gain versus time for 4340 steel in the presence of  $$\rm SO_2$  moist (98% R.H.). Microbalance and chamber results.

Values of weight gains, weight losses and corrosion rates for steel 4340 in the presence of  ${\rm SO}_2$ -moist (49% R.H.). Microbalance and chamber results. Table 12.

	CH	CHAMBER (4 samples)	(sa	MICI	MICROBALANCE (1 sample)	ample)
Time	Weight Gain	Weight Loss	Corrosion Rate	Weight Gain	Weight Loss	Corrosion Rate
(hours)	(mg)	(mg)	(mm/year)	(Bm)	(mg)	(mm/year)
80	0.300	0.375	1.227	0.320		
16	0.475	0.725	1.125	0.532		
24	0.625	0.975	1.064	0.764		
32				0.872		
40				966.0		
48	0.925	1.025	0.672	1.132		
56				1.256		
<b>79</b>				1.380		
72	1.425	1.300	0.472	1.548	1.412	0.513

Values of weight gains, weight losses and corrosion rates for steel 4340 in the presence of  $\rm SO_2$ -moist (98% R.H.). Microbalance and chamber results. Table 13.

nmple)	Corrosion Rate (mm/year)									0.873
MICROBALANCE (1 sample)	Weight Loss (mg)									2.400
MICE	Weight Gain (mg)	0.512	0.851	1.224	1.395	1.593	1.811	2.009	2.208	2.520
(s	Corrosion Rate (mm/year)	1.964	1.800	1.609			1.050			0.816
CHAMBER (4 samples)	Weight Loss (mg)	0.600	1.100	1.475			1.925			2.244
СН	Weight Gain (mg)	0.475	0.750	1.125			1.675			2.375
	Time (hours)	80	16	24	32	40	48	56	79	72



Weight gain versus time for 4340 steel in the presence of moist SO<sub>2</sub> (98% R.H.) (curve A), and moist air (98% R.H.) (curve B). Microbalance and chamber results. Figure 14.

give sulfuric acid, which attacks the iron giving ferrous sulfate; this is now oxidazed to produce ferric sulfate which hydrolyzes to produce ferric hydroxide liberating sulfuric acid, which now acts on further iron according with the reaction:

Fe 
$$\frac{\text{H}_2\text{SO}_4 + \frac{1}{2}\text{O}_2}{\text{FeSO}_4}$$
 FeSO<sub>4</sub>  $\frac{\frac{1}{4}\text{O}_2 + \frac{1}{2}\text{H}_2\text{SO}_4}{\text{1}_2\text{Fe}_2\text{O}_3 + 3/2 \text{H}_2\text{SO}_4}$  (5)

In the electrochemical cycle, the mechanism involves anodic and cathodic reactions and once that ferric hydroxide and ferrous sulfate are present on the surface of the metal, ferric rust (FeOOH) can be reduced to magnetite ( $\text{Fe}_3\text{O}_4$ ) at the cathodic points, whereas at the anodic points iron passes into the liquid as  $\text{Fe}^{2+}$  ions. Magnetite formed cathodically can be oxidized by air to give fresh ferric rust in a greater amount compared with the amount that had been present before. The reactions can be written as follows:

$$Fe \rightarrow Fe^{2+} + 2e$$
 (anodic reaction) (16)

8FeOOH + Fe<sup>2+</sup> + 2e 
$$\rightarrow$$
 3Fe<sub>3</sub>0<sub>4</sub> + 4H<sub>2</sub>0 (cathodic reaction) (17)

$$3\text{Fe}_3^{0}_4 + 3/4 \, 0_2 + 9/2 \, \text{H}_2^{0} \rightarrow 9\text{FeOOH (reoxidation)}$$
 (18)

this cycle increases the amount of rust since 8Fe00H becomes 9Fe00H.

Taylor (17) found that both reactions can take place, but once ferric hydroxide and ferrous sulfate are present, the electrochemical cycle proceeds faster than the acid regeneration cycle.

After 72 hours of exposure, samples of 4340 steel presented a dark film of corrosion products with formation of small droplets on the surface indicating the probability of the presence of the acid

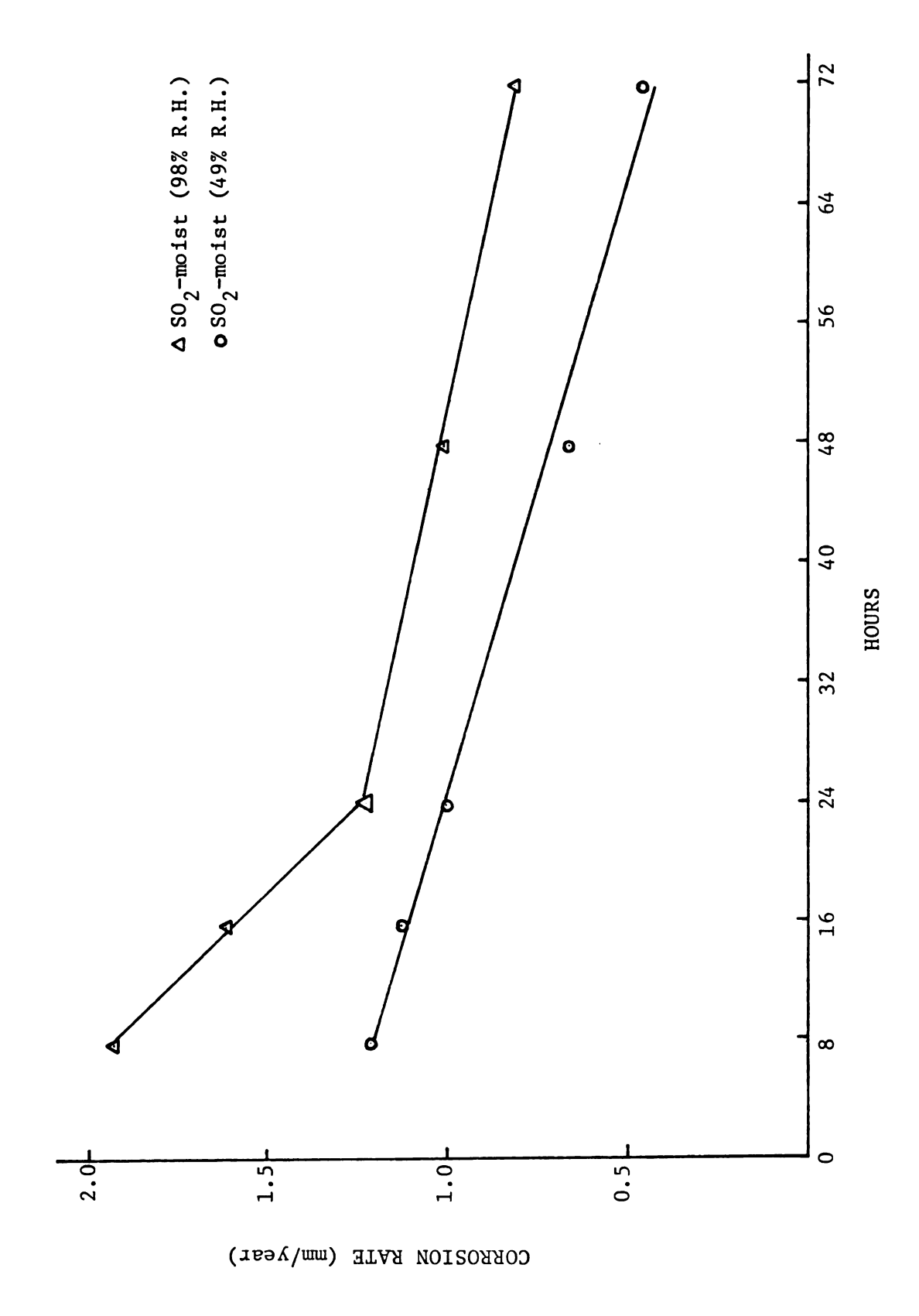
regeneration cycle. This phenomenon was observed to be more intense in the moist  $\mathrm{SO}_2$  test at 98% relative humidity than in the moist  $\mathrm{SO}_2$  test at 49% relative humidity; these results are illustrated in Fig. 15 where the plots of corrosion rates versus time show an important difference, giving always higher values in the moist  $\mathrm{SO}_2$  test at 98% relative humidity.

## B. Magnesium Alloy AZ31B

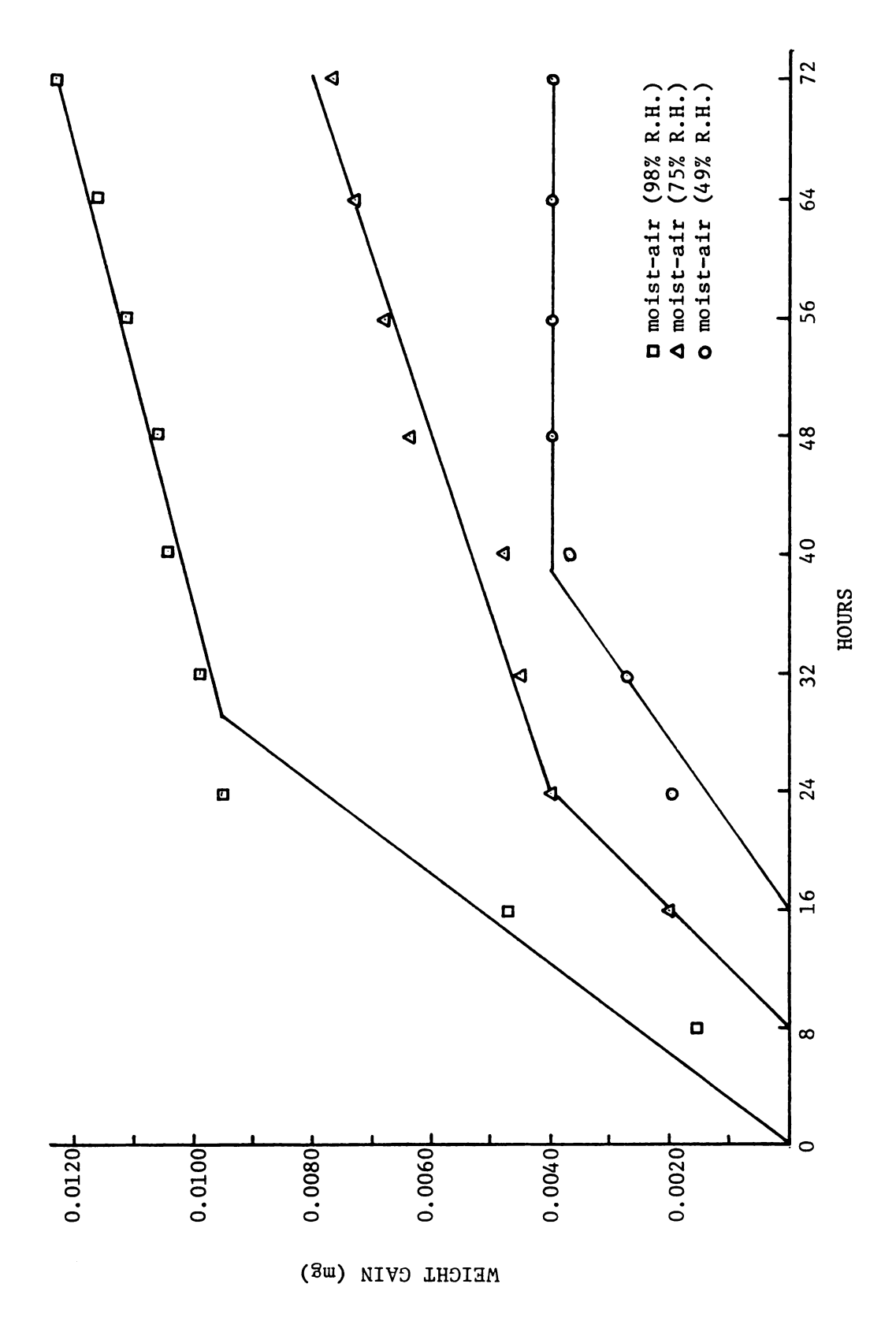
1. Moist Air Tests. Fig. 16 shows weight gain versus time for magnesium alloy AZ31B in moist air at 49%, 75% and 98% relative humidity obtained from microbalance tests. Tables 14, 15 and 16 show the values of weight gain, weight loss and corrosion rate for magnesium alloy AZ31B in moist air at 49%, 75% and 98% relative humidity obtained from both microbalance and chamber tests.

From the Tables it is observed that there were no values detected at all for any of the chamber tests. This was attributed to the fact that the Mettler balance used in all the chamber tests was not sensitive enough to measure the small changes in weight gain and weight loss suffered by magnesium AZ31B under moist air conditions. For this reason, only microbalance results were used in this part of the experiment.

From Fig. 16 it is noticed that in general magnesium AZ31B has a very good resistance to moist air conditions, even at high relative humidity. An induction period with no weight gain was also observed in the case of atmospheres containing 49% and 75% relative humidity. This induction period extended for 16 hours in the presence of moist air at 49% relative humidity; it is also important to note that



Corrosion rates versus time for 4340 steel in the presence of moist  $\mathrm{SO}_2$  (98% R.H.) and moist  $\mathrm{SO}_2$  (49% R.H.). Chamber results. Figure 15.



Weight gain versus time for magnesium AZ31B in the presence of moist air (49%, 75% and 98% R.H.). Microbalance results. Figure 16.

Values of weight gains, weight losses and corrosion rates for magnesium AZ31B in the presence of moist-air (49% R.H.). Microbalance and chamber results. Table 14.

ımple)	Corrosion Rate (mm/year)									900.0
MICROBALANCE (1 sample)	Weight Loss (mg)									0.0040
MICF	Weight Gain (mg)	0.0	0.0	0.0020	0.0027	0.0037	0.0040	0,0040	0.0040	0.0040
(s)	Corrosion Rate (mm/year)	0.0	0.0	0.0			0.0			0.0
CHAMBER (4 samples)	Weight Loss (mg)	0.0	0.0	0.0			0.0			0.0
CH7	Weight Gain (mg)	0.0	0.0	0.0			0.0			0.0
	Time (hours)	æ	16	24	32	40	48	26	99	72

Table 15. Values of weight gains, weight losses and corrosion rates for magnesium AZ31B

results.	.sample)	ss Corrosion Rate (mm/year)									0.0126
and chamber	MICROBALANCE (1 sample)	Weight Loss (mg)									0.0077
. Microbalance	MICI	Weight Gain (mg)	0.0	0.0020	0,0040	0.0045	0.0048	0.0064	0.0068	0.0073	0.0077
in the presence of moist-air (75% R.H.). Microbalance and chamber results	(Sa	Corrosion Rate (mm/year)	0.0	0.0	0.0			0.0			0.0
presence of moi	CHAMBER (4 samples)	Weight Loss (mg)	0.0	0.0	0.0			0.0			0.0
in the	СН	Weight Gain (mg)	0.0	0.0	0.0			0.0			0.0
		Time (hours)	œ	16	24	32	40	87	56	79	72

Values of weight gain, weight loss and corrosion rate for magnesium AZ31B in the presence of moist air (98% R.H.). Microbalance and chamber results. Table 16.

sample)	Corrosion Rate	(mm/year)									0.0203
MICROBALANCE (1 sample)	Weight Loss	(gm)									0.0124
MIC	Weight Gain	(Sm)	0.0016	0.0048	9600.0	0.0100	0.0105	0.0107	0.0112	0.0117	0.0124
(sa)	Corrosion Rate	(mm/year)	0.0	0.0	0.0			0.0			0.0
CHAMBER (4 samples)	Weight Loss	(gm)	0.0	0.0	0.0			0.0			0.0
The state of the s	Weight Gain	(gm)	0.0	0.0	0.0			0.0			0.0
	Time	(hours)	∞	16	24	32	0 7	87	99	79	72

under these conditions the weight gain remained constant during the last 24 hours of exposure, indicating the protective nature of the corrosion products in preventing further corrosion.

At 75% relative humdity, the induction period decreased in 8 hours and the corrosion products did not show a protective behavior.

As in the case of 4340 steel, it seems that the critical relative humidity for magnesium AZ31B appears at a relative humidity between 75% and 98% at which the samples started to corrode more rapidly. Under these conditions the samples showed small changes in weight from the beginning of the test, and there was no induction period present. At this relative humidity, the corrosion products did not show a protective nature according to the trace of the weight gain-time curve. From these facts it is clear that the corrosion rate of magnesium AZ31B is a direct function of the relative humidity present.

After 72 hours of exposure, the samples did not show change in color or appearance in any of the circumstances described above, retaining a lustruous surface during all the test.

In summary, the results here obtained show that magnesium AZ31B has a very good corrosion resistance in uncontaminated moist atmospheres.

These results are in good agreement with reports found in the literature (2, 3, 55-58).

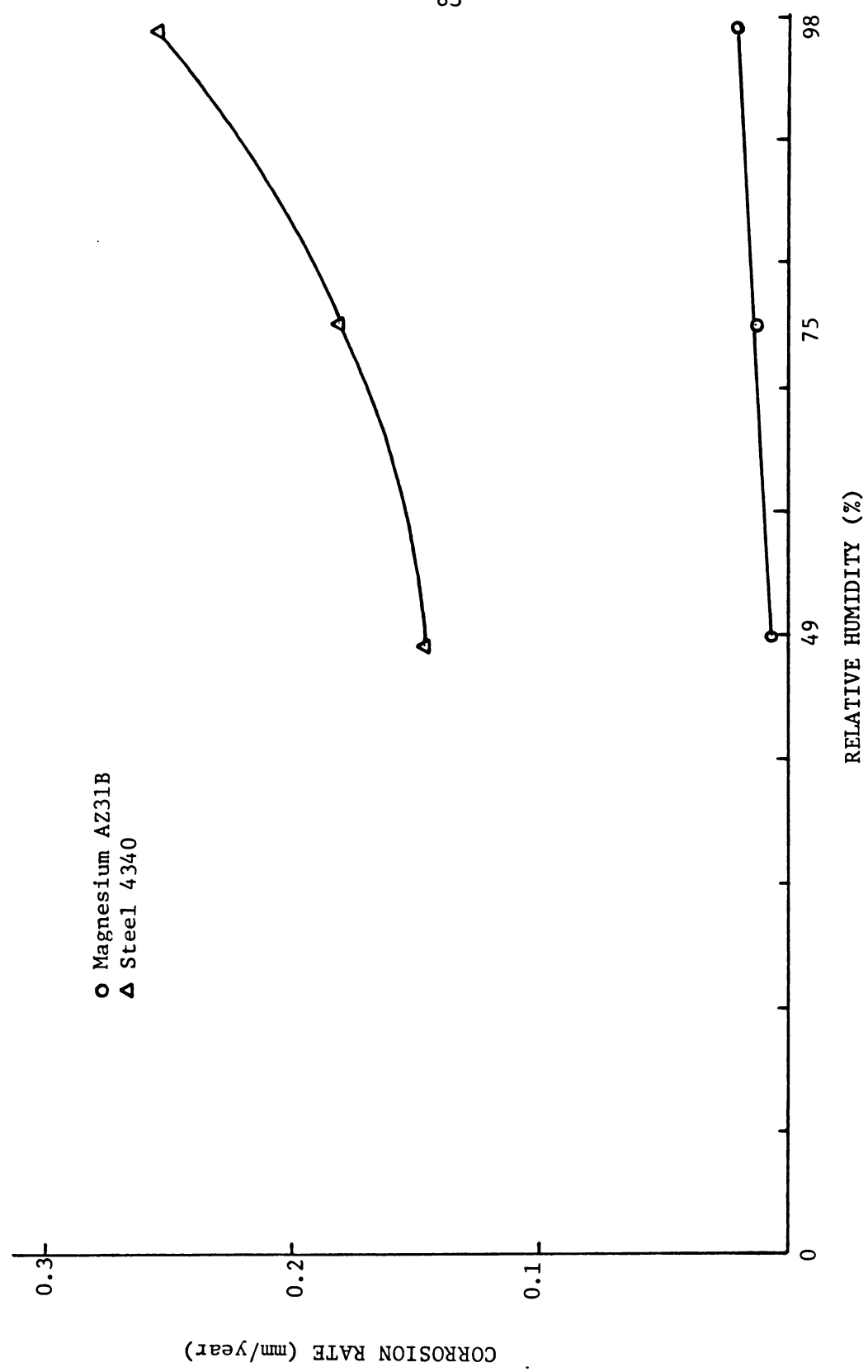
The good resistance to moist air conditions is attributed to the formation of an oxide film that is highly protective (57); this film produced by the interaction of magnesium with moist air, appears to be essentially magnesium hidroxide, especially when magnesium is exposed to 93% and higher relative humidities (2, 55, 56, 57). This insoluble hydroxide film is found to be formed according with the reaction:

$$Mg + 2H_2O \rightarrow Mg(OH)_2 + H_2$$
 (19)

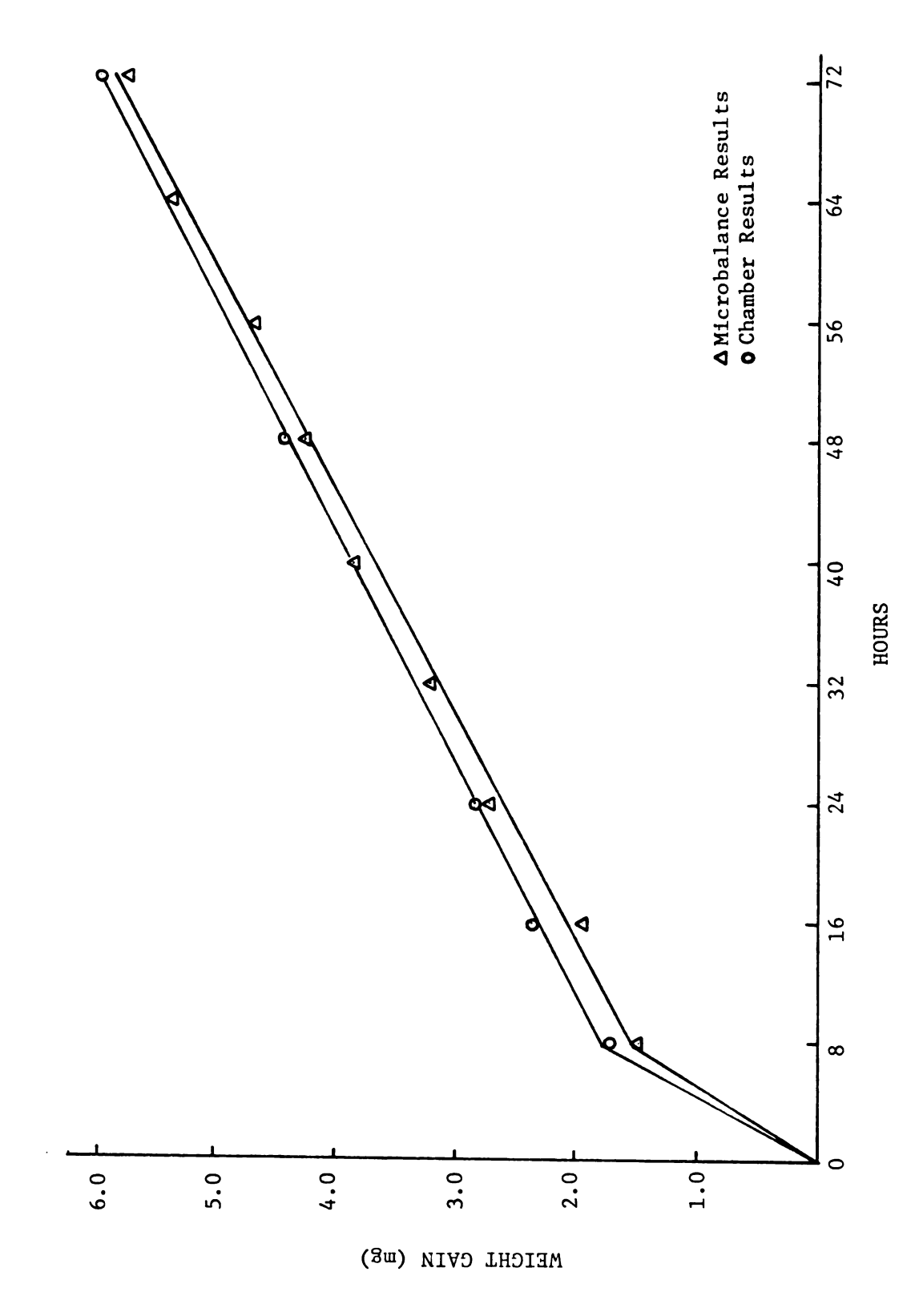
It is important to mention that the surface film contains a higher percentage of the hydroxides of the alloying metals (aluminum and zinc hydroxides in our case) than would be expected from the composition of the alloy (57). It has been established (58) that when a magnesium alloy contains aluminum as in the case of AZ31B alloy, hydrotalcite  $^{\rm Mg}_6$  Al $_2$  (OH) $_{16}$  CO $_3$  · 4H $_2$ O, which has a ratio of 1 aluminum atom to 4 magnesium atoms, concentrates in the film of corrosion products. This concentration of aluminum provides the film with very good dissolution resistance properties, being this the probable reason of the improved resistance to weathering of magnesium alloy AZ31B.

- Fig. 17 shows the comparative effects of relative humidity in the corrosion rates of 4340 steel and magnesium AZ31B. As it has already been discussed earlier, corrosion rates are higher when the relative humidity is increased, this effect being more notorious in 4340 steel than in magnesium AZ31B, for the case of uncontaminated atmospheres.
- 2. Dry SO<sub>2</sub> Tests. Fig. 18 shows weight gain versus time for magnesium AZ31B in dry SO<sub>2</sub> obtained from both microbalance and chamber tests. Table 17 shows the values of weight gain, weight loss and corrosion rate for the same conditions. From Fig. 18 it is observed that the weight gain of samples after 72 hours of exposure was extremely high with a poor protective film of corrosion products. Comparing the results obtained in moist air at 98% relative humidity shown in Table 16 with the results obtained in the dry SO<sub>2</sub> test shown in Table 17 we find that the weight gain under dry SO<sub>2</sub> conditions is almost 500 times higher than when samples were exposed 72 hours to moist air at 98% relative humidity.





Corrosion rates versus relative humidity for 4340 steel and magnesium AZ31B after 72 hours of exposure. Microbalance and chamber results. Figure 17.



Weight gain versus time for magnesium AZ31B in the presence of dry  $\mathrm{SO}_2$ . Microbalance and chamber results. Figure 18.

Values of weight gain, weight loss and corrosion rate for magnesium AZ31B in the presence of dry  ${\rm SO}_2$ . Microbalance and chamber results. Table 17.

umple)	Corrosion Rate (mm/year)									10.942
MICROBALANCE (1 sample)	Weight Loss (mg)									6.612
MICR	Weight Gain (mg)	1.428	1.974	2.736	3,420	3.813	4.248	4.710	5.265	5.728
s)	Corrosion Rate (mm/year)	33.238	20.312	17.234			12.925			11.489
CHAMBER (4 samples)	Weight Loss (mg)	2.250	2.750	3.500			5.250			7.000
CHT	Weight Gain (mg)	1.700	2,350	2.850			4.425			6.000
	Time (hours)	œ	16	24	32	07	87	56	79	72

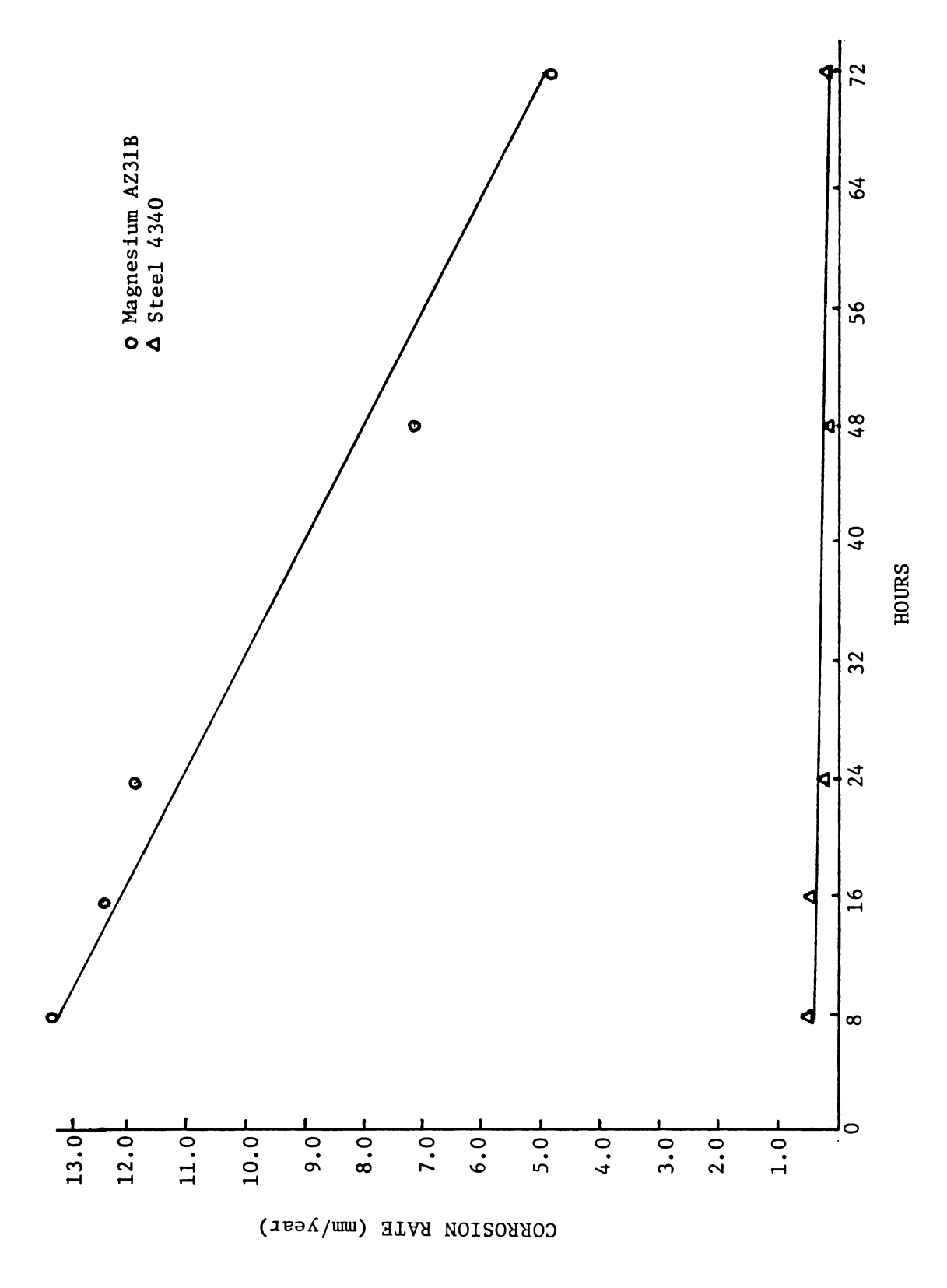
After exposure, a grey film of corrosion products, probably composed of magnesium sulfite (MgSO<sub>3</sub>) or magnesium sulfate (MgSO<sub>4</sub>) (56). was observed on the surface of the metal. When the samples were withdrawn from the chamber and from the microbalance, small droplets started to form all over the surface indicating the hygroscopic nature of the corrosion products. These formation of droplets took place immediately after the samples were exposed to the humidity present in the laboratory.

These results do not agree with literature (56) where it is stated that sulfur dioxide causes no attack in magnesium alloys at ordinary temperatures. Nevertheless, it is very likely that the dissolution of the film of corrosion products is attributable to the presence of dust or other hygroscopic particles on the metal surface (2).

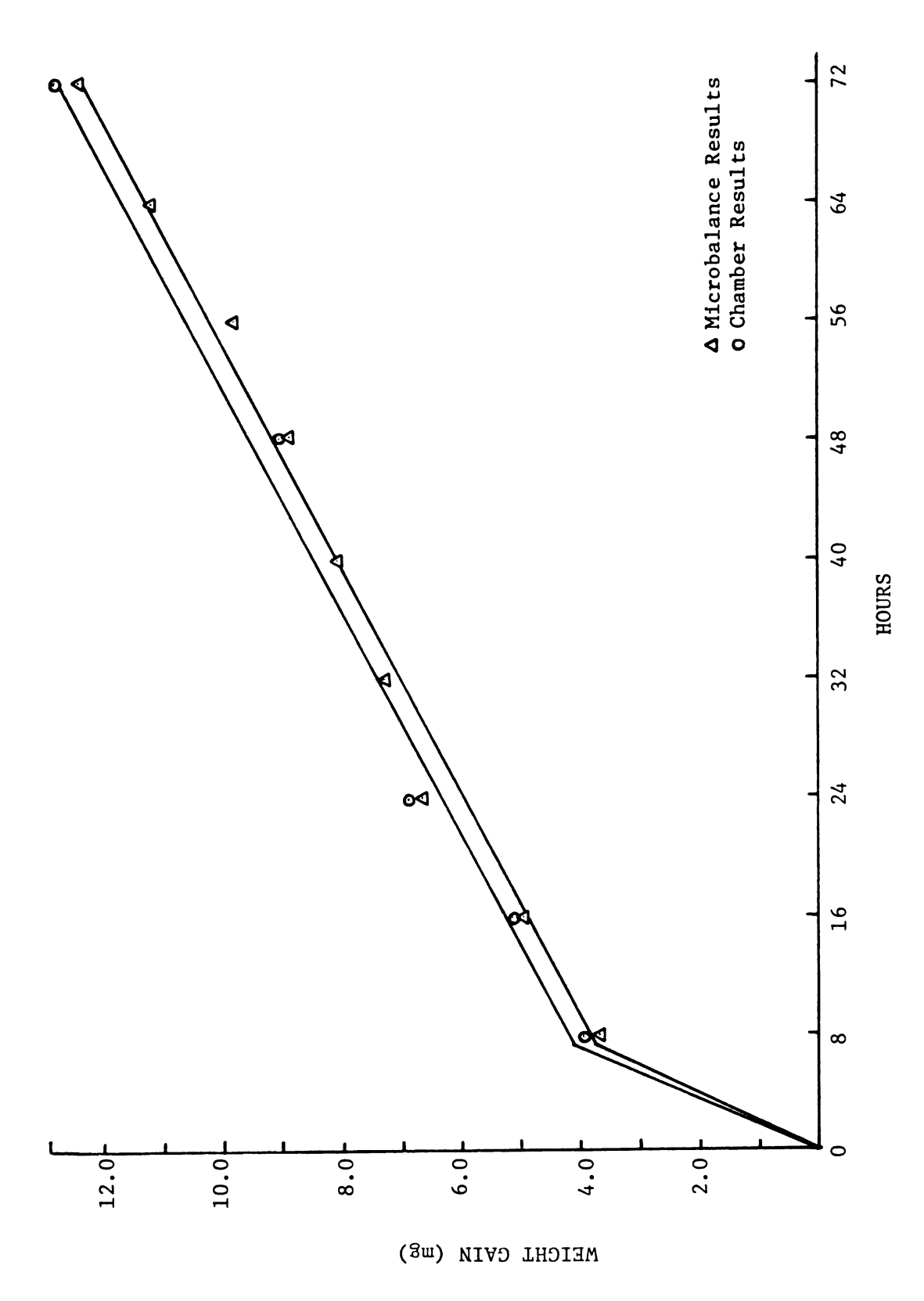
Fig. 19 shows corrosion rates versus time for 4340 steel and magnesium AZ31B in the presence of dry SO<sub>2</sub> obtained from chamber tests. It is evident that although the corrosion products formed in 4340 steel present some degree of dissolution, they tend to be more protective against further attack that the soluble corrosion products formed on the surface of magnesium AZ31B.

3. Moist  $\mathrm{SO}_2$  Tests. Figs. 20 and 21 show weight gain versus time for magnesium AZ31B in moist  $\mathrm{SO}_2$  at 49% and 98% relative humidity obtained from both microbalance and chamber tests. Tables 18 and 19 show the values of weight gain, weight loss and corrosion rate for magnesium AZ31B in moist  $\mathrm{SO}_2$  at 49% and 98% relative humidity obtained from both microbalance and chamber tests.

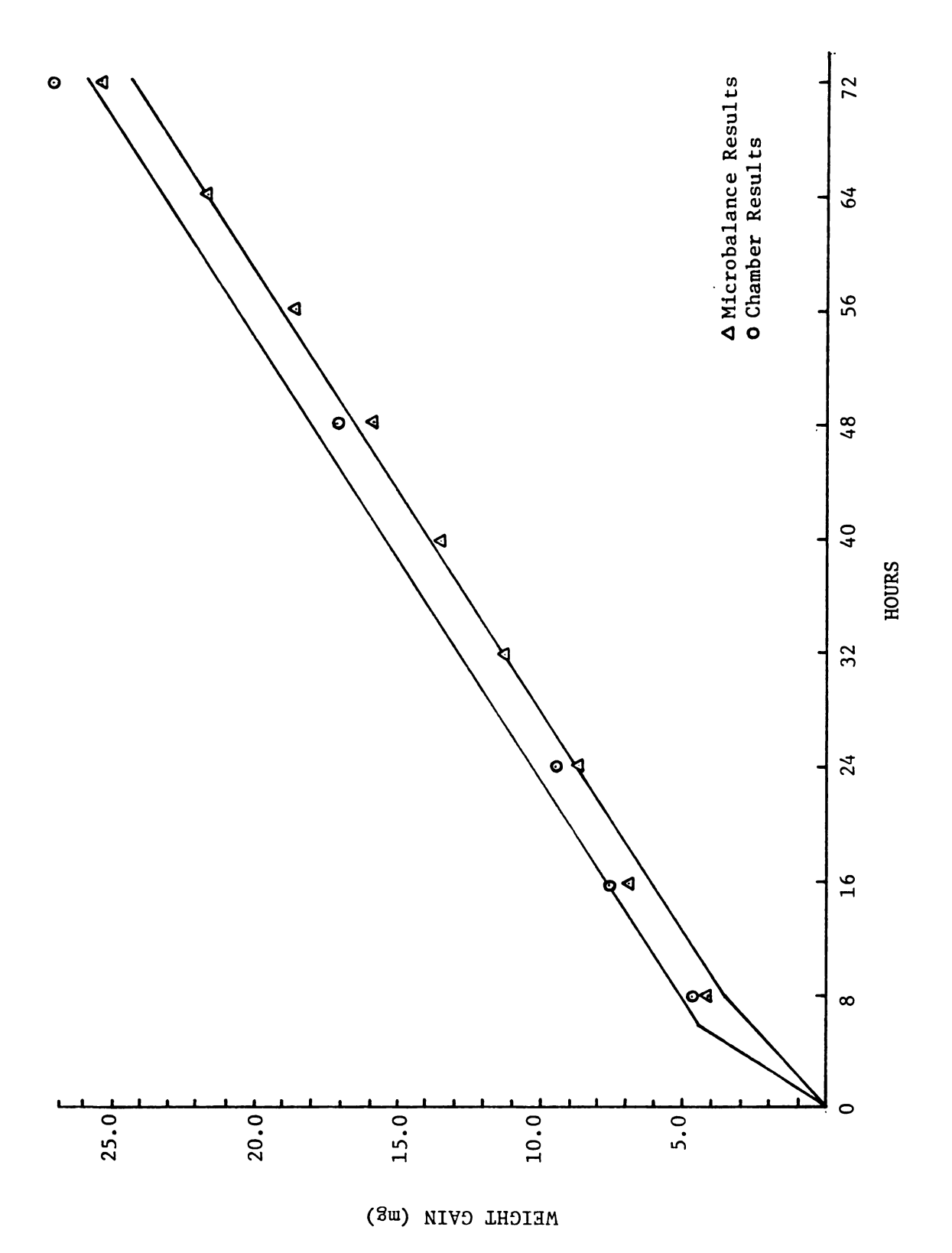
It can be observed from the figures the great increase in weight gain and consequently in corrosion rate, suffered by magnesium AZ31B when



Corrosion rates versus time for 4340 steel and magnesium AZ31B in the presence of dry  ${\rm SO}_2$ . Microbalance and chamber results. Figure 19.



Weight gain versus time for magnesium AZ31B in the presence of moist  ${\rm SO}_2$  (49% R.H.). Microbalance and chamber results. Figure 20.



Weight gain versus time for magnesium AZ31B in the presence of moist  ${\rm SO}_2$  (98% R.H.). Microbalance and chamber results. Figure 21.

Values of weight gain, weight loss and corrosion rate for magnesium AZ31B in the presence of moist  ${\rm SO}_2$  (49% R.H.). Microbalance and chamber results. Table 18.

	CH7	CHAMBER (4 samples)	(8:	MICI	MICROBALANCE (1 sample)	umple)
Time	Weight Gain	Weight Loss	Corrosion Rate	Weight Gain	Weight Loss	Corrosion Rate
(hours)	(mg)	(mg)	(mm/year)	(mg)	(mg)	(mm/year)
<b>&amp;</b>	4.000	5.400	79.772	3.760		
16	5.190	7.000	51.708	5.044		
24	6.920	9.300	45.791	6.725		
32				7.398		
40				8.124		
87	9.026	12.107	29.840	8.932		
99				9.820		
99				11.296		
72	12.850	14.825	24.246	12.418	14.293	23.460

Values of weight gain, weight loss and corrosion rate for magnesium AZ31B in the presence of moist  ${\rm SO}_2$  (98% R.H.). Microbalance and chamber results. Table 19.

	MICROBALANCE (1 sample)
	samples)
	CHAMBER (4 samples)

Time	Weight Gain	Weight Loss	Corrosion Rate	Weight Gain	Weight Loss	Corrosion Rate
(hours)	(mg)	(mg)	(mm/year)	(mg)	(mg)	(mm/year)
8	4.800	6.500	96.023	4.364		
16	7.750	10.400	76.814	7.046		
24	009.6	12.000	59.099	8.808		
32				11,488		
40				13.642		
87	17.300	20.750	51.117	16.080		
99				18.762		
79				21.886		
72	27.200	29.900	49.075	25.514	28.040	46.024

exposed to a moist air containing sulfur dioxide atmosphere. It is clear that the presence of sulfur dioxide even at very low relative humidities provokes a pronounced attack on the metal surface. It was found (See Tables 16 and 19) that the weight gain was in the order of several thousand times higher when the values for the moist SO<sub>2</sub> test at 98% relative humidity were compared with the values of the moist air test at 98% relative humidity, indicating that the corrosion products formed on the surface of the metal do not have a protective action against further attack.

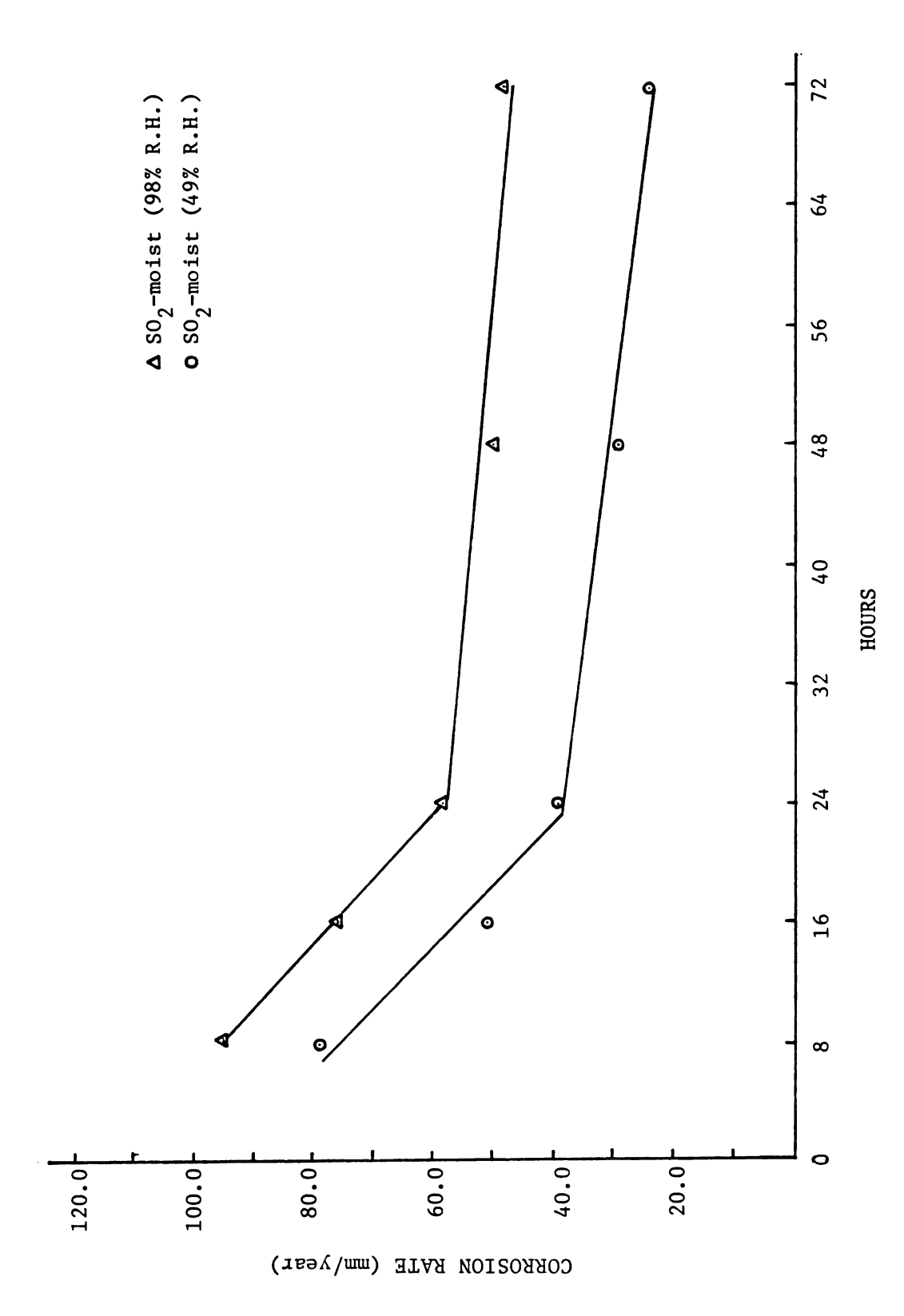
As in the case of the dry  $SO_2$  test, a greyish film of corrosion products was formed on the metallic surface, and for both moist  $SO_2$  at 49% relative humidity and moist  $SO_2$  at 98% relative humidity tests, a liquid film appeared over the surface even before the samples were withdrawn from the test atmosphere, being an indication of the high solubility of the corrosion products formed, which are very likely to be composed of magnesium sulfate (MgSO<sub>4</sub>) and magnesium hydroxide (MgOH<sub>2</sub>) (56).

After the cleaning procedure used for removing the corrosion products, it was found that small pits had formed in a uniform manner all over the metal surface. It has been established (57) that pitting in magnesium results from two possible ways: a) foreign materials or particles present in the metal itself or in the film of corrosion products are cathodic to magnesium causing localized pitting, b) as a result of the type of pitting known as "pinhole" pitting, which takes place in points on the surface of the metal where the protective film is broken, such points being anodic to the surrounding cathodic area where the film is in good conditions.

It appears that the formation of pits can be attributed to the first of these mechanisms since it is possible that dust particles were present on the metal surface at the moment the tests were performed.

Fig. 22 shows corrosion rates versus time form magnesium AZ31B in the presence of moist SO<sub>2</sub> at 49% and 98% relative humidity. As in the case of 4340 steel higher corrosion rates were obtained at 98% relative humidity with the formation of droplets on the sample surface.

In general, it is very difficult to make significative comparisons between the results here obtained and results already published in the atmospheric corrosion of 4340 steel and magnesium alloy AZ31B because of variability in the conditions under which the tests reported were performed. The main points that account for the variations in the results obtained are: differences in length of exposure time, differences in sample size, differences in conditions of exposure and in some cases differences in cleaning procedures. Tables 20 and 21 show comparisons between the results obtained in this experiment and the results reported by Pelensky and Jaworski (34) and Summitt and Fink (4) for 4340 steel and magnesium alloy AZ31B. The values of weight loss that appear in both tables were obtained from the corrosion rates reported by these investigators and using Equation (15). Although a significative comparison between the reported results and the results obtained in this experiment cannot be made, it can be observed from these tables that according with the results reported by Pelensky and Jaworski and the results here obtained, corrosion rates decrease with time under the same exposure conditions.



Corrosion rates versus time for magnesium AZ31B in the presence of moist  ${\rm SO}_2$  (49% R.H.), and moist  ${\rm SO}_2$  (98% R.H.). Chamber results. Figure 22.

Comparisons between the results obtained in this experiment and the results steel. According with the corrosion severity classification system used by reported by Pelensky and Jaworski (34) and Summitt and Fink (4) for 4340 Summitt and Fink, a severe atmosphere corresponds to an environment with high moisture content together with low pollutant content. Table 20.

Results by	Atmosphere	Exposure Time (hours)	Corrosion Rate (mm/year)	Sample Area (cm <sup>2</sup> )	Weight Loss (gr)
Laboratory	moist air (98% R.H.) 24	R.H.) 24	0.300	0.426	0.000275
Laboratory	moist air (98%	(98% R.H.) 48	0.272	0.426	0.000500
Laboratory	moist air (98% R.H.) 72	R.H.) 72	0.254	0.426	0.000700
Pelensky-Jaworski	Tropical	1464	0.069	9.677	0.086162
Pelensky-Jaworski	Tropical	2880	0.055	9.677	0.137360
Pelensky-Jaworski	Tropical	5760	0.037	9.677	0.184812
Pelensky-Jaworski	Tropical	10944	0.046	9.677	0.436556
Pelensky-Jaworski	Tropical	17520	0.048	9.677	0.731256
Summitt-Fink	Severe	52560	0.0046	181.610	3.934000
Summitt-Fink	Severe	43800	0.0058	181.610	4.134000
Summitt-Fink	Severe	52560	0,0060	181.610	5.132000

Comparisons between the results obtained in this experiment and the results reported by Pelensky and Jaworski (34) and Summitt and Fink (4) for magnesium AZ31B. According with the corrosion severity classification system used by Summitt and Fink, a severe atmosphere corresponds to an environment with high moisture content together with low pollutant content. Table 21.

Results by	Atmosphere	Exposure Time (hours)	Corrosion Rate (mm/year)	Sample Area $(cm^2)$	Weight Loss (gr)
Laboratory	moist air (98% R.H.)	.н.) 72	0.0203	0.426	0.000124
Pelensky-Jaworski	Tropical	1464	0.0310	9.677	0.008580
Pelensky-Jaworski	Tropical	2880	0.0370	9.677	0.020482
Pelensky-Jaworski	Tropical	5760	0.0340	9.677	0.037643
Pelensky-Jaworski	Tropical	10944	0.0250	9.677	0.052590
Pelensky-Jaworski	Tropical	17520	0.0280	9.677	0.094551
Summitt-Fink	Severe	52560	0.0050	181.610	0.948000
Summitt-Fink	Severe	43800	0.0074	181.610	1.169000
Summitt-Fink	Severe	52560	0.0107	181.610	2.028000

## VI. CONCLUSIONS

A laboratory system based on a continuous reading technique for assessing atmospheric corrosion has been designed, assembled and tested. Determination of the progress of corrosion products with time was measured by means of a Cahn electrobalance model RG.

Comparisons of weight gain with time between microbalance and static environmental chamber in the atmospheric corrosion of low alloy high strength steel 4340 and magnesium alloy AZ31B exposed to a number of different environments, have shown that continuous reading techniques with a microbalance are useful for rapid corrosion testing.

Both microbalance and chamber methods showed that the corrosion rate of 4340 steel and magnesium alloy AZ31B in a moist atmosphere depends on the relative humidity present. Higher corrosion rates were observed as relative humidity was increased. Corrosion rates decreased with time of exposure, however, for all the cases, indicating the protective nature of the corrosion products formed on the metal surface. Magnesium AZ31B showed very good corrosion resistance even at 98% relative humidity. A critical relative humidity was detected for 4340 steel and magnesium AZ31B at some point between 75% and 98% relative humidity were corrosion started to proceed more rapidly. These results are in agreement with previously established values for both metals.

Dry sulfur dioxide produced an increase in corrosion rate for both metals with respect to those found in the moist air tests. These results do not agree with published results in which it was reported that dry SO<sub>2</sub> does not produce a significant attack on the metal. This disagreeement could be attributed to the presence of humidity in the laboratory when the tests were performed.

As expected, moist SO<sub>2</sub> atmosphere caused the most severe attack on both 4340 steel and magnesium AZ31B, this effect being slightly more marked at higher relative humidities with the formation of a liquid film on the corrosion products layer.

Under these conditions, it was difficult to determine a critical relative humidity since corrosion rates were very high at even 45% relative humidity, which is below the critical humidity cited in the literature of 60% for the case of steels in sulfur dioxide-containing environments.

In general, corrosion rates in 4340 steel and magnesium AZ31B increased with the severity of the exposure conditions. For the case of magnesium AZ31B the corrosion rate differences when exposed to moist air with and without sulfur dioxide was remarkable, indicating that magnesium AZ31B has a very good corrosion resistance in non-contaminated atmospheres. On the other hand, it is severely attacked when contaminants are present. This inconsistency in behavior has been attributed to the different nature of the corrosion products formed on the surface of the metal.

Comparisons between the results here obtained and results already published in the atmospheric corrosion of 4340 steel and magnesium AZ31B proved to be of no help for assessing the reliability of the system, mainly because of variability in the conditions of the tests reported in the literature, especially in field tests, and lack in the

controllability of certain variables in the present system such as sulfur dioxide concentrations.

For this reason, some changes to the original design are suggested in order to have a better control of the environmental conditions produced in the laboratory. The changes proposed are basically two:

- 1. The addition of a wet-bulb psychrometric apparatus for continuously measuring humidity. The apparatus consists of two thermometers placed in close proximity. The bulb of one is housed in a wick saturated with water (wet bulb) whereas the other is left completely open to the gas flow. The gas flow cools the wet bulb thermometer to a new equilibrium temperature, and the relative humidity can then be obtained by knowing the dry-bulb temperature and difference between the dry and wet-bulb temperatures.
- 2. To provide the system with a gas-detector apparatus which would allow to control and measure a broad range of gas concentrations from sulfur dioxide and dilution gas cylinders.

In summary, the continuous reading technique using a microbalance has proven to be very useful for assessing atmospheric corrosion in the laboratory. This technique showed these advantages.

- a) The sample weight is recorded continuously, permitting the determination of the actual weight gained by the sample throughout the test.
- b) The microbalance worked very well in the presence of the counterflow of dry air used for keeping the highly corrosive sulfur dioxide away from the weighing mechanism.

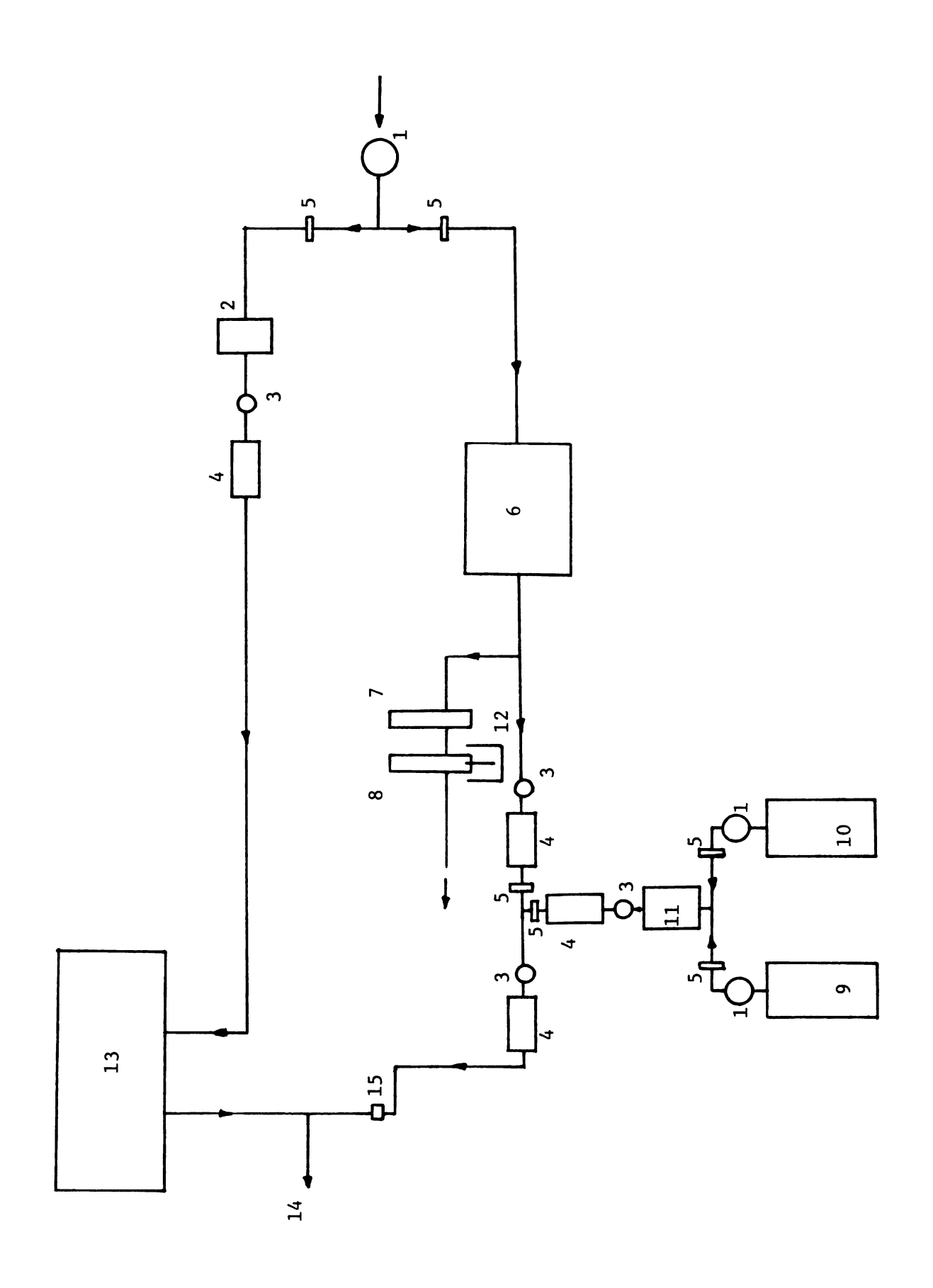
c) The high sensitivity of the microbalance allowed to measure very small changes in weight. This advantage was particularly useful in the measurement of weight gains of magnesium AZ31B in the moist air tests, where the Mettler balance was unable to detect these small changes.

APPENDIX I.

## APPENDIX I.

Figure 23. Schematic diagram of the system showing the changes suggested in order to achieve better reproduction of environmental conditions in the laboratory.

- 1. Low pressure regulators
- 2. "Drierite" tower
- 3. Needle valves
- 4. Flowmeters
- 5. Control valves
- 6. Gas-dispersion bottle
- 7. Dry-bulb thermometer
- 8. Wet-bulb thermometer
- Sulfur dioxide cylinder with a concentration in air of
   50 999 parts per million
- 10. Dilution-gas cylinder
- 11. Gas-detector system for determining concentrations
- 12. Distilled water bottle
- 13. Cahn RG electrobalance
- 14. Gas discharge
- 15. Sample



LIST OF REFERENCES

## LIST OF REFERENCES

- 1. Tomashov, N. D., "Theory of Corrosion and Protection of Metals," McMillan, New York, NY, 1966.
- 2. Shreir, L. L., "Corrosion," Vol. 1, John Wiley & Sons, Inc., New York, NY, 1963.
- 3. Uhlig, H. H., "Corrosion and Corrosion Control," John Wiley & Sons, Inc., New York, NY, 1971.
- 4. Summitt, R., and Fink, F. T., "PACER LIME: An Environmental Corrosion Severity Classification System," Technical Report, Air Force Materials Laboratory, Wright Patterson AFB, OH, 1980.
- 5. Haynie, F. H., and Upham, J. B., "Correlation Between Corrosion Behavior of Steel and Atmospheric Pollution Data," "Corrosion in Natural Environments, ASTM STP 558," American Society for Testing and Materials, pp. 33-51, 1974.
- 6. Sereda, P. J., "Weather Factors Affecting the Corrosion of Metals,"
  "Corrosion in Natural Environments, ASTM STP 558," American Society for
  Testing and Materials, pp. 7-22, 1974.
- 7. Scully, J. C., "The Fundamentals of Corrosion," Pergamon Press, Oxford, England, 1975.
- 8. Vernon, W. H., in "Transactions," Faraday Society, Vol. 27, pp. 265-277, 1931.
- 9. Sereda, P. J., "Measurement of Surface Moisture and Sulfur Dioxide Activity at Corrosion Sites," ASTM Bulletin, American Society for Testing and Materials, No. 246, pp. 47-48, 1960.
- 10. Guttman, H., and Sereda, P. J., "Measurement of Atmospheric Factors Affecting the Corrosion of Metals," "Metal Corrosion in the Atmosphere, ASTM STP 435," American Society for Testing and Materials, pp. 326-359, 1968.
- 11. Guttman, H., "Effects of Atmospheric Factors on the Corrosion of Rolled Zinc," "Metal Corrosion in the Atmosphere, ASTM STP 435," American Society for Testing and Materials, pp. 223-239, 1968.
- 12. Grossman, P. R., "Investigation of Atmospheric Exposure Factors That Determine Time of Wetness of Outdoor Structures," "Atmospheric Factors Affecting the Corrosion of Engineering Metals, ASTM STP 646," American Society for Testing and Materials, pp. 5-16, 1978.

- 13. Samsami, N., and Summitt, R., unpublished results.
- 14. Rozenfeld, I. L., "Atmospheric Corrosion of Metals," National Association of Corrosion Engineers, Houston, TX, 1972.
- 15. Engel, R. E., Goerke, W. H., and Saygin, R., "Air Quality Criteria for Sulfur Oxides," Technical Report, NATO Expert Panel on Air Quality Criteria, Brussels, Belgium, 1971.
- 16. Haynie, F. H., Spence, J. W., and Upham, J. B., "Effects of Air Pollutants on Weathering Steel and Galvanized Steel: A Chamber Study," "Atmospheric Factors Affecting the Corrosion of Engineering Metals, ASTM STP 646," American Society for Testing and Materials, pp. 30-47, 1978.
- 17. Evans, U. R., "The Corrosion and Oxidation of Metals," Edward Arnold Publishers, London, England, 1976.
- 18. Evans, U. R., "The Corrosion and Oxidation of Metals," Edward Arnold Publishers, London, England, 1961.
- 19. Wranglen, G., in Corrosion Science, Vol. 9, pp. 585-590, 1969.
- 20. Fryburg, G. C., and Kohl, F. J., "Hot Corrosion Studies of Four Nickel-Base Superalloys: B-1900, NASA-TRW VIA, 713C and IN738," Procedures of the Symposium on Properties of High Temperature Alloys with Emphasis on Environmental Effects, Electrochemical Society, pp. 585-594, 1976.
- 21. Huang, T., Gulbransen, E. A., and Meier, G. H., "Hot Corrosion of Ni-Base Turbine Alloys in Atmospheres in Coal-Conversion Systems," Journal of Metals, Vol. 31, No. 3, pp. 28-35, 1979.
- 22. Hutchings, R., and Loretto, M. H., "Compositional Dependence of Oxidation Rates of NiAl and CoAl," Metal Science, Vol. 12, No. 11, pp. 503-510, 1978.
- 23. Gulbransen, E. A., "Oxidation Studies with the Vacuum Microbalance in Complex Environments," Journal of Vacuum Science Technology, Vol. 17, No. 1, pp. 109-113, 1980.
- 24. Murray, P. J., "Simultaneous Acquisition of Mossbauer Spectra and Microbalance Data in Situ: A Possible New Technique for the Study of Iron Corrosion and Oxidation," British Corrosion Journal, Vol. 12, No. 3, p. 192, 1977.
- 25. Rice, D. W., Phipps, B. P., and Tremoureux, R., "Atmospheric Corrosion of Cobalt," Journal of the Electrochemical Society, Vol. 126, No. 9, pp. 1459-1466, 1979.
- 26. Volrabova, H., and Vlasakova, L., "Piezoelectric Microbalance and its Use in the Study of Volatile Inhibitors," British Corrosion Journal, Vol. 3, No. 3, pp. 76-79, 1968.
- 27. Rozenfeld, I. L., and Enikeev, E. K., "Effect of Volatile Corrosion Inhibitors on Water Vapor Adsorption on Iron," Protection of Metals, Translated from Zashchita Metallov, Vol. 10, No. 5, pp. 491-493, 1974.

- 28. Lee, W. Y., and Eldridge, J., "Oxidation Studies of Permalloy Films by Quartz Crystal Microbalance, AES, and XPS," Journal of the Electrochemical Society, Vol. 124, No. 11, pp. 1747-1751, 1977.
- 29. Lee, W. Y., Siegmann, H. C., and Eldridge, J., "A Comparison of the Mass and Resistance Change Techniques for Investigating Thin Film Corrosion Kinetics," Journal of the Electrochemical Society, Vol. 124, No. 11, pp. 1744-1747, 1977.
- 30. Sharma, S. P., "Reaction of Copper and Copper Oxide with H<sub>2</sub>S," Journal of the Electrochemical Society, Vol. 127, No. 1, pp. 21-26, 1980.
- 31. Li, K., and Rogan, F. H., "Study of the Mechanism of the Hydrogen Sulfide/Dolomite Reaction," Technical Report, United States Department of Energy, 1978.
- 32. Brandt, S. M., and Adam, L. H., "Atmospheric Exposure of Light Metals," "Metal Corrosion in the Atmosphere, ASTM STP 435," American Society for Testing and Materials, pp. 95-128, 1968.
- 33. Ailor, W. H., "Seven-Year Exposure at Point Reyes, California," "Corrosion in Natural Environments, ASTM STP 558," American Society for Testing and Materials, pp. 75-81, 1974.
- 34. Pelensky, M. A., Jaworski, J. J., and Gallaccio, A., "Corrosion Investigations at Panama Canal Zone," "Atmospheric Factors Affecting the Corrosion of Engineering Metals, ASTM STP 646," American Society for Testing and Materials, pp. 58-73, 1978.
- 35. Pearlstein, F., and Teitell, L., "Corrosion and Corrosion Prevention of Light Metal Alloys," CORROSION /73, Anaheim, CA, 1973.
- 36. Mannweiler, G. B., "Corrosion Test Results on Fifteen Ferrous Metals After Seven-Years Atmospheric Exposure," "Metal Corrosion in the Atmosphere, ASTM STP 435," American Society for Testing and Materials, pp. 211-222, 1968.
- 37. Briggs, C. W., "Atmospheric Corrosion of Carbon and Low Alloy Cast Steels," "Metal Corrosion in the Atmoshere, ASTM STP 435," American Society for Testing and Materials, pp. 271-284, 1968.
- 38. Haynie, F. H., and Upham, J. B., "Effects of Atmospheric Pollutants on Corrosion Behavior of Steels," Materials Performance, Vol. 10, No. 11, pp. 18-21, 1971.
- 39. Barton, K., in "Werkstoffe und Korrosion," Vol. 20, No. 3, p. 216, 1969.
- 40. Spence, J. W., and Haynie, F. H., "Design of a Laboratory Experiment to Identify the Effects of Environmental Pollutants on Materials," "Corrosion in Natural Environments, ASTM STP 558," American Society for Testing and Materials, pp. 279-291, 1974.
- 41. Cahn, L., and Schultz, H. R., "The Cahn Recording Gram Electrobalance," Vacuum Microbalance Techniques, Vol. 3, pp. 29-44, 1963.

- 42. Rockland, L. B., "Saturated Salt Solutions for Static Control of Relative Humidity Between 5 and 40° C," Analytical Chemistry, Vol. 32, No. 10, pp. 1375-1376, 1960.
- 43. Perry, R. H., and Chilton, C. H., "Chemical Engineer's Handbook," McGraw-Hill, New York, NY, 1973.
- 44. Secrist, J. H., and Powell, W. H., "General Chemistry." Van Nostrand Company Publishers, Princeton, NJ, 1966.
- 45. Sathyanarayana, R., "Low Temperature Oxidation Kinetics of Single Crystal Zinc," Ph. D. Thesis, Michigan State University, 1970.
- 46. "Metals Handbook Vol. 8," "Metallography, Structures and Phase Diagrams," American Society for Metals, Metals Park, OH, 1973.
- 47. "Metals Handbook Vol. 7," "Atlas of Microstructures," American Society for Metals, Metals Park, OH, 1973.
- 48. Pedersen, E., "A Symmetrical Vacuum Thermobalance for Corrosive Atmospheres," Journal of Scientific Instruments, Vol. 1, pp. 1013-1015, 1968.
- 49. "Standard Method G 1," "Part 10, ASTM Book of Standards," American Society for Testing and Materials, Philadelphia, PA, 1980.
- 50. Champion, F. A., "Corrosion Testing Procedures," John Wiley & Sons, Inc., New York, NY, 1952.
- 51. Upham, J. B., "Atmospheric Corrosion Studies in Two Metropolitan Areas," Journal of the Air Pollution Control Association, Vol. 17, No. 6, pp. 398-402, 1967.
- 52. Vernon, W. H., "The Corrosion of Metals in Air," Chemistry and Industry, Vol. 62, No. 8, pp. 314-318, 1943.
- Hauffe, K., "Oxidation of Metals," Plenum Press, New York, NY, 1965.
- 54. Kubaschewski, O., and Hopkins, B. E., "Oxidation of Metals and Alloys," Butterworths Publishers, London, England, 1962.
- 55. Uhlig, H. H., "Corrosion Handbook," John Wiley & Sons, Inc., New York, NY, 1948.
- 56. "Metals Handbook Vol. 1," "Properties and Selection of Metals," American Society for Metals, Metals Park, OH, 1973.
- 57. LaQue, F. L., and Copson, H. R., "Corrosion Resistance of Metals and Alloys," Reinhold Publishing Corporation, New York, NY, 1963.
- 58. Godard, H. P., "The Corrosion of Light Metals," John Wiley & Sons, Inc., New York, NY, 1967.

